Electronic Supplementary Material (ESI) for Materials Advances.

Impact of subtle change in branched amino acid on the assembly and properties of perylene bisimides hydrogels

Jacquelyn G. Egan[a], Glen Brodie[a], Daniel McDowall[a], Andrew J. Smith[b], Charlotte J. C. Edwards-Gayle and Emily R. Draper[a*]

[a]School of Chemistry, Joseph Black Building, University of Glasgow, Glasgow, G12 8QQ, UK

[b]Diamond Light Source Ltd, Harwell Science and Innovation Campus, Didcot, OX11 0QX, U.K.

*Corresponding author** Emily.Draper@glasgow.ac.uk

SUPPORTING INFORMATION

Table of Contents

1. Synthesis and General Procedures

1.1 Synthesis and Characterization

All chemicals were purchased from Merck Life Science or Alfa Aesar and used without further purification. Deionised water was used throughout.

All PBI-amino acid molecules were synthesized as previously reported, with the characterization data matching that reported.[1–4]

1.2 N, N'-di(L-isoleucine)-perylene-3,4:9,10-tetracarboxylic acid bismide (PBI-I) synthesis

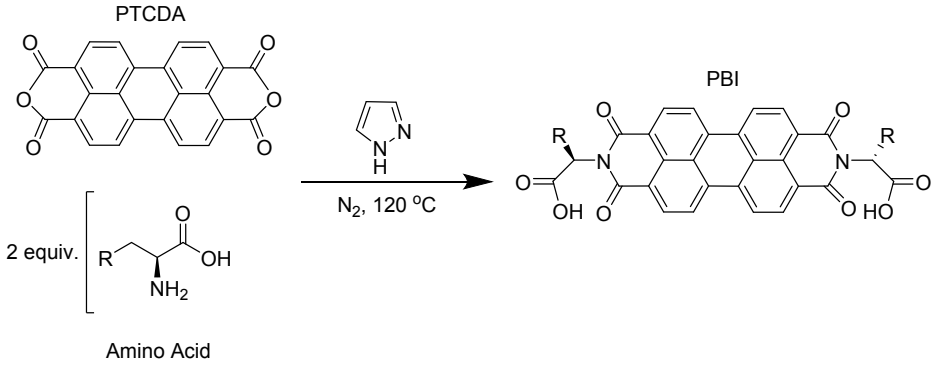

Scheme S1. *General reaction scheme for an imide substitution for an amino acid substituted PBI*

In a round bottom flask, imidazole (16.3 g, 240 mmol, 30 equiv.) was heated at 120ºC until molten and then stirred. To the imidazole was added 3,4:9,10-perylenetetracarboxyldianhydride (PTCDA) (3.13 g, 8.00 mmol, 1 equiv.) and L-Isoleucine (2.1 g, 16 mmol, 2 equiv.). The flask was placed under an atmosphere of nitrogen and allowed to stir for 5 h at 130ºC. The reaction was then quenched with 2 M HCl and filtered. The cake was then allowed to air dry overnight, before being resuspended in water and boiled for 20 minutes to remove residual imidazole. The suspension was then filtered, and the solid was heated to 60ºC under vacuum to remove volatiles. This resulted in **PBI-I** as a dark purple solid (4.24 g, 86% yield). All the other PBI materials were prepared in this way but have been previously reported. The yield obtained for all the PBIs was between 70-90%

^{1}H-NMR 400 MHz, DMSO-*d*$_6$, 25ºC: δ (ppm) = 8.24 – 7.92 (m, 8H), 5.26 (dd, J = 9.0, 2.2 Hz, 1H), 5.22 (d, J = 9.0 Hz, 1H), 2.62 – 2.48 (m, 2H), 2.05 – 1.92 (m, 1H), 1.41 – 1.28 (m, 2H), 1.24 (d, J = 6.4 Hz, 3H), 1.02 (t, J = 7.4 Hz, 3H), 1.02 – 0.98 (m, 1H), 0.84 (t, J = 7.3 Hz, 3H), 0.77 (d, J = 6.9 Hz, 3H).

^{13}C-NMR 100 MHz, DMSO-d$_6$, 25ºC: δ (ppm) = 170.7 (COOH); 162.3 (C=O); 133.4, 131.0, 128.0, 124.8, 123.3, 121.5 (perylene core); 57.6 (CH), 56.3 (CH), 33.2 (CH), 33.1 (CH), 27.9 (CH_2); 24.9 (CH_2); 18.1 (CH_3); 14.8 (CH_3); 11.2 (CH_3); 11.0 (CH_3).

FT-IR: v/cm^{-} 3171b (O-H), 1698s (C=O), 1595s (C=O), 1331s (C-O), 1179s (C-O), 805s (aromatic C-H), 745 (aromatic C-H).

ESI-TOF MS: calculated 641.19 Da for $[C_{36}H_{30}N_2NaO_8]^+$, found 641.18 Da ($C_{36}H_{30}N_2NaO_8$). CHN Anal. for $C_{36}H_{30}N_2O_8$ Calcd: C, 69.89; H, 4.89; N, 4.53. Found C, 67.67; H, 4.92; N, 4.61.

2. Methods

2.1 Characterization of PBIs

All the nuclear magnetic resonance (NMR) spectra were measured using a Bruker DPX-400 spectrometer operating at 400 MHz for ^{1}H-NMR and 100 MHz for ^{13}C-NMR in d_6 DMSO. The Infrared (IR) spectroscopy was collected using a Thermo Nicolet Is5 (Diamond ATR attachment). The spectra were recorded at 64 scans and a resolution of 4 cm^{-1}. The background was of the empty ATR crystal and spectra were recorded of the PBIs as solid powders. Mass spectrometry was performed using a Bruker MicroTOF mass spectrometer using electrospray ionization (MS-ESI). TGA and DTG was carried out on a TGA SDT Q500 V6.7 Build 203 TGA machine using a constant nitrogen flow of 100 mL/min. Samples were heated to 610°C at a heating rate of 10°C/min.

2.2 Preparation of Solutions of PBIs

Solutions were prepared using a concentration of 10 mg/mL of PBI. For the preparation of a 5 mL solution with a concentration of 10 mg/mL, 50 mg of PBI was weighed into a vial. An equimolar amount of sodium hydroxide (0.1 M, aqueous) was added to the PBI and then was made up to 5 mL with water. For 5 mL solutions with concentrations of 2.5 mg/mL to 15 mg/mL preparation the method was the same with the initial amount changing (12.5 mg to 75 mg) and an equimolar amount of sodium hydroxide (0.1 M, aqueous) was added to the PBI and then was made up to 5 mL with water. The solution was stirred for at least 16 hours to allow all the PBI to dissolve. A large stock solution of each PBI was prepared to ensure that the solutions were the same for each experiment. The pH of each vial was then adjusted as necessary using 2 M HCl or 2 M NaOH to get the desired pH. All preparation of samples was carried out at room temperature (around 25ºC in the daytime).

2.3 Preparation of PBI gels

All the hydrogels were formed using a pH switch and at a concentration of 10 mg/mL of gelator solution as described above. 2 mL of the gelator solution, prepared as described above, was then transferred to a 7 mL Sterlin vial that contained a pre-weighed amount of glucono-δ-lactone (GdL) and shaken gently. This was left to stand for at least 16 hours to allow for gelation to occur. All preparation of samples was done at room temperature (around 25ºC in the daytime). After 16 hours if the samples were stable to inversion this suggestion that gelation may have occurred. These samples could then be rheologically tested for confirmation of gelation.

The pH was checked for the solution before and after gelation to check that the difference was not due to difference in pH. Measurements were performed in triplicate and errors were calculated from the standard deviation.

2.4 Small Angle X-ray Scattering (SAXS) Data

Samples for scattering were prepared by making stock solutions of the PBIs with a concentration of 10 mg/mL and one equimolar amount of sodium hydroxide (0.1 M, aqueous) and allowing it to stir overnight. Then aliquots of the stock solution were put into a 7 mL Sterlin vials and the pH was adjusted to the desired values using either 2 M HCl or 2 NaOH. A capillary tube was filled three-quarters with the solution at desired pH and sealed with a plastic lid and parafilm to prevent leaks or change in the pH. For the hydrogels, an aliquot of stock solution was added to a 7 mL Sterlin vial that contained a pre-weighed amount of GdL and shaken gently. A capillary tube was filled three-quarters with the mixture and sealed with a plastic lid and parafilm to then left to sit for 16 hours to allow for gelation.

Scattering data was collected at I22, under experiment number SM27906-1, using a beam energy of 12.4 keV and a sample to detector distance of 5.647m calibrated using a standard sample of silver behenate. Data was collected as a single frame of 1s duration and reduced to a 1-d dataset using the DAWN software package and standard pipelines.[5,6]

The scattering length density of each material was calculated using the National Institute of Standard and technology Neutron activation and scattering calculator.[7]

Table S1. *Calculated scattering length density for different PBIs used.*

PBI	X-ray scattering length density / $Å^{-2}$
-L	$13.826 \cdot 10^{-6}$
-I	$13.826 \cdot 10^{-6}$
-V	$13.769 \cdot 10^{-6}$

The data were fitted to models in the Sasview software package (version).[8] Various models were used to fit the data. Fitting errors are provided as ±; the errors were obtained from the fitting software and do not consider other sources of error. These compounds are expected to form 1D fibres at low pH and they can form worm-like micelles structures at high pH.[3,9] Previous fitting of similar structures have been reported and found cylindrical models were appropriate.[10–12] Fitting the data to different cylinder models was attempted to find the most suitable, starting from models with fewer parameters to the more complex ones. A model was deemed suitable based on the reduced Chi^2, a Chi^2 below 5 was deemed suitable. Generally, the model with the lowest Chi^2 was chosen unless there were regions of the fit that clearly were not representative of the data set. In some cases, single models were not suitable to achieve a good fit, indicating a co-existence of structures. In these instances, models were combined using the “Easy Sum/Multi(p1, p2) editor” in the SasView software. The combined model could then be saved and used in the same manner as any other. In the results tables from the fitting shown below, a “+” sign is used to denote where two models were combined. In some of the data, fitting to a single model was attempted and if a low enough reduced Chi^2 could not be obtained, a combined model was attempted. For PBIs at different pH there were a few cases where a suitable model could not be obtained. In those cases, pH was around 5-6 and we attributed the

high Chi^2 values and poor fits to a transition period. During this transition period the structure are varied and cannot be described by the models in SASview. Listed are tables with attempted fits for those cases to highlight the difficulty fitting. At high pH, lower scattering structures are present that are best fit to a spherical model combined with a form of cylindrical model or power law.

2.5 Rheological Measurements

Dynamic rheological and viscosity measurements were performed using an Anton Par Physica MCR301 rheometer. Strain and frequency data were collected using a vane (ST10-4V-8.8/97.5) and cup geometry so that samples could be prepared in 7 mL Sterlin vials to remove any loading issues. Viscosity and time sweep data were collected using a 50 mm cone (cone angle 0.994°) geometry and temperature controlled bottom plate. Time sweeps were collected used a 50 mm sandblasted parallel plate. All measurements were collected in triplicate and at 25°C.

2.5.1 Viscosity measurements

A 1 mL aliquot of PBI solution with the desired concentration or at the desired pH was pipetted on the bottom plate. The plate lowered on top of the solution to a gap height of 0.1 mm which is determined for the cone angle on the plate. Any excess sample was trimmed using a metal spatula. Ensuring no gaps or bubbles on the edge of the plate. A CP50 plate geometry was used to measure the viscosity. Measurements were recorded at a shear rate from 0.1-1000% and performed in triplicate and errors were calculated from the standard deviation.

2.5.2 Strain Sweeps

Strain sweeps were recorded from 0.1-1000% strain at set frequency of 10 rad/s with a gap height of 2 mm. Samples were prepared as described previously in a 7 mL Sterlin vial. Measurements were performed in triplicate and errors were calculated from the standard deviation.

2.5.3 Frequency Sweeps

Frequency scans were recorded from 1 rad/s to 100 rad/s under a constant strain of 0.5% with a gap height of 2 mm. The strain was chosen because it is in the linear viscoelastic region for the hydrogels. Samples were prepared as described previously in a 7 mL Sterlin vial. Measurements were performed in triplicate and errors were calculated from the standard deviation.

2.5.4 Time Sweeps

Time sweeps were measured with an angular frequency of 10 rad/s with a strain of 0.5%. Samples were prepared as described previously in a 7 mL Sterlin vial then pipette on the bottom plate. A sandblasted CP50 plate geometry was used to measure the time sweep. The plate lowered on top of the solution to a set gap height of 0.8 mm. Any excess sample was trimmed using a mental spatula. The plate was flooded with mineral oil to prevent the gel from drying whilst gelling

2.6 UV-vis Absorption Spectroscopy Measurements

All the UV-vis absorption spectra were measured using an Agilent Cary 60 spectrometer. For the initial spectra of the PBIs, the samples were made by taking a stock solution of the PBIs with a concentration of 10 mg/mL at pH = 7 and placing them in a 0.1 mm cuvette and measuring between 200 nm to 1100 nm on medium scan rate. Gel samples were made by adding 2 mL of PBI 10 mg/mL solution was added to GdL in a 7 mL Sterlin vial and 0.5 mL was pipetted to a 0.1 mm cuvette then parafilmed and left to stand for at least 16 hours to allow for gelation to occur. Then measuring between 200 nm to 1100 nm on medium scan rate. To form radical, the samples where irradiated at 365 nm with a LED light for 5 minutes.

The molar absorptivity was calculated for each PBI by measuring a dilution series of the stock solutions of PBIs. There are two different values for the molar absorptivity for the two strongly absorbing S_0–S_1 transition peaks. The error was calculated with the flitted slope for the plotted data.

The UV-vis absorption spectra of the PBIs at different pH were measured by taking a stock solution of PBI with a concentration of 10 mg/mL and disturbing aliquots to five 7 mL Sterlin vials. The pH of each vial was then adjusted as necessary using 2 M HCl or 2 M NaOH to get the desired pH.

2.7 pH Measurements

pH measurements were recorded using a custom-built pH/temperature logger and a HANNA pH probe (FC200) specifically for gels with a given error of ±0.1. For monitoring the pH of gelation over time, 2 mL of PBI solution was added to GdL in a 7 mL Sterlin vial and this was immersed in a water bath at a set temperature of 25°C. The probe tip was then inserted into the gel with parafilm used to seal the top of the vial/tip. The pH measurements were recorded every 30 seconds for between 14 to 18 hours until gelation was complete, and pH had stabilized.

2.8 Apparent pK_a titrations

pH measurements were recorded using a custom-built pH/temperature logger pH probe with a given error of ±0.1. For pK_a measurements, 2 mL of PBI solution was added to a 7 mL Sterlin vial which was immersed in a water bath at a set temperature of 25°C and the probe was immersed in the solution. 5 µL – 10 µL aliquots of HCl (0.1M) were added to the solution with the pH recorded after the reading had stabilized. The solution was gently stirred between additions of acid to avoid any gel forming and to ensure the pH was homogeneous through the solution. The plateaus in the data represent the apparent pK_a values.

2.9 Cyclic Voltammetry (CV)

CVs for the solutions were collected using a three-electrode system and a Palmsense potentiostat with a glassy carbon working electrode, a Pt wire counter electrode and an Ag/AgCl reference electrode. The background electrolyte was 0.1 M NaCl in water, and then 0.1 M tetrabutylammonium hexafluoroborate (TBAHFB) in MeCN. The

measurements were scanned from 1.0 V to -1.0 V at a scan rate 0.05 V/s and measured in triplicate. The clearest scan from the three scans at 0.05 V/s were used for analysis.

For calibration, the $E_{1/2}$ for the ferrocene-ferrocecium redox couple (Fc/Fc^+) in MeCN was measured at 0.359 V vs Ag/AgCl. Although not used for the calibration, the $E_{1/2}$ for the ferrocene carboxylic acid redox couple (Fc-COOH/Fc^+-COOH) in MeCN was measured at 0.559 V vs Ag/AgCl.

CVs for the hydrogels were collected using a two-electrode system and a Palmsense potentiostat. The hydrogels were prepared by taking a 2 mL aliquot of 10 mg/mL solution and adding it to a vial containing 8 mg/mL GdL. The solution was then poured into a 1.5 mm O-ring on top of a 5 x 5 cm fluorine doped tin oxide (FTO) glass and another piece of FTO glass of the same size was placed on top. The device was held together using claps and allowed to sit overnight. The CVs were measured the next day, one FTO glass was used as the working electrode while the other was used as the reference/counter electrode. The background electrolyte was 0.1 M NaCl in water, and then 0.1 M tetrabutylammonium hexafluoroborate (TBAHFB) in MeCN. The measurements were scanned from 2.0 V to -3.5 V at a scan rate 0.1 V/s and measured in triplicate. The clearest scan from the three scans at 0.1 V/s were used for analysis.

For calibration, the $E_{1/2}$ for the ferrocene-ferrocecium redox couple (Fc/Fc^+) in MeCN was measured at -0.66 V. Although not used for the calibration, the $E_{1/2}$ for the ferrocene carboxylic acid redox couple (Fc-COOH/Fc^+-COOH) in MeCN was measured at 0.56 V.

2.10 ^{1}H-NMR Kinetics

^{1}H-NMR spectra were measured using a Bruker DPX-400 spectrometer operating at 400 MHz with the temperature internally controlled. Samples were run in D_2O/NaOD with a capillary standard of 0.1% polydimethylsiloxane (PDMS) in tetrachloroethylene solution as a reference. First the standard was added to a 1 mL of PBI solution with a concentration of 10 mg/mL and a spectrum collected prior to the addition of GdL, this is the time zero measurement (t=0). Next, 8 mg of GdL was added to the remaining 1 mL of PBI solution with standard then added to the NMR tube and inserted into the spectrometer. Due to experimental limitation, there was 5-10 minutes time delay between the addition of the sample to the instrument and the first measurement. Spectra were recorded every 5 minutes until the PBI's protons peaks were no longer detectable. This took 4-5 hours depending on the sample. Example spectra recorded over time are shown in the figures below for clarity. The PDMS reference proton environment was integrated and set to the same value in all the spectra. The protons for the PBIs were then integrated and compared to the integration value for the same PBIs peaks at t = 0. When assembled the PBIs become NMR invisible and that can be detected as the percentage un-assembled. From this the percent assembled was calculated and a trend was plotted against time.

3. Data

3.1 Synthetic characterization

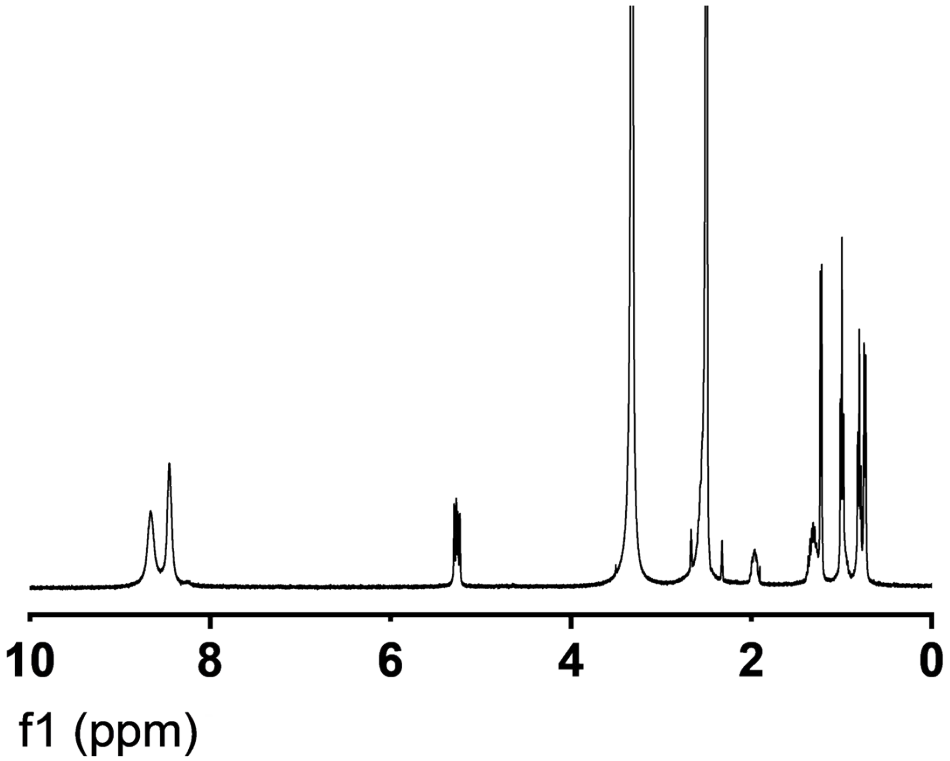

Figure S1. *^{1}H-NMR spectrum of **PBI-I** in DMSO-d_6 at 25ºC*

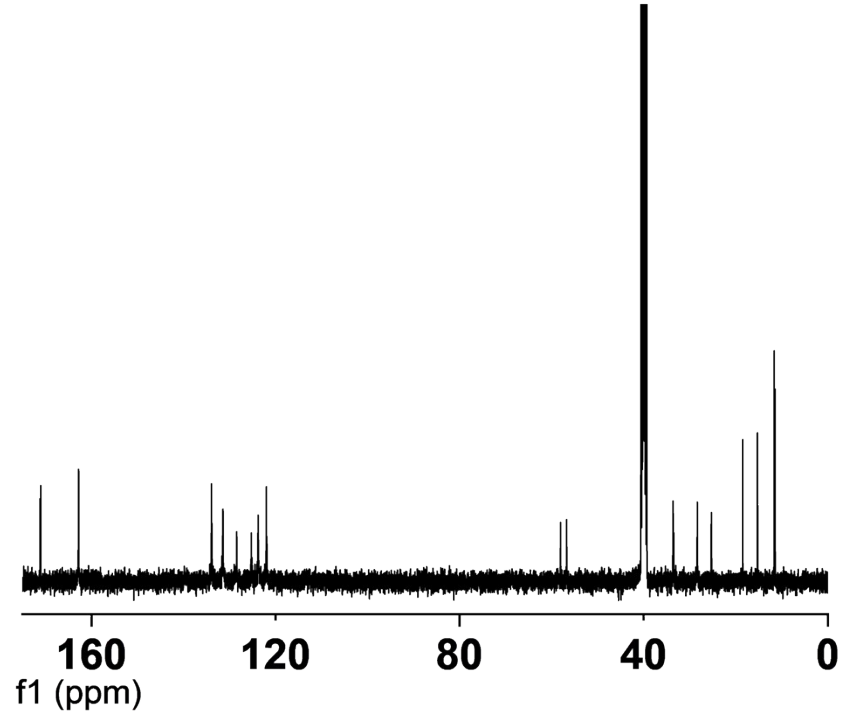

***Figure S2**. ^{13}C-NMR spectrum of **PBI-I** in DMSO-d_6 at 25ºC*

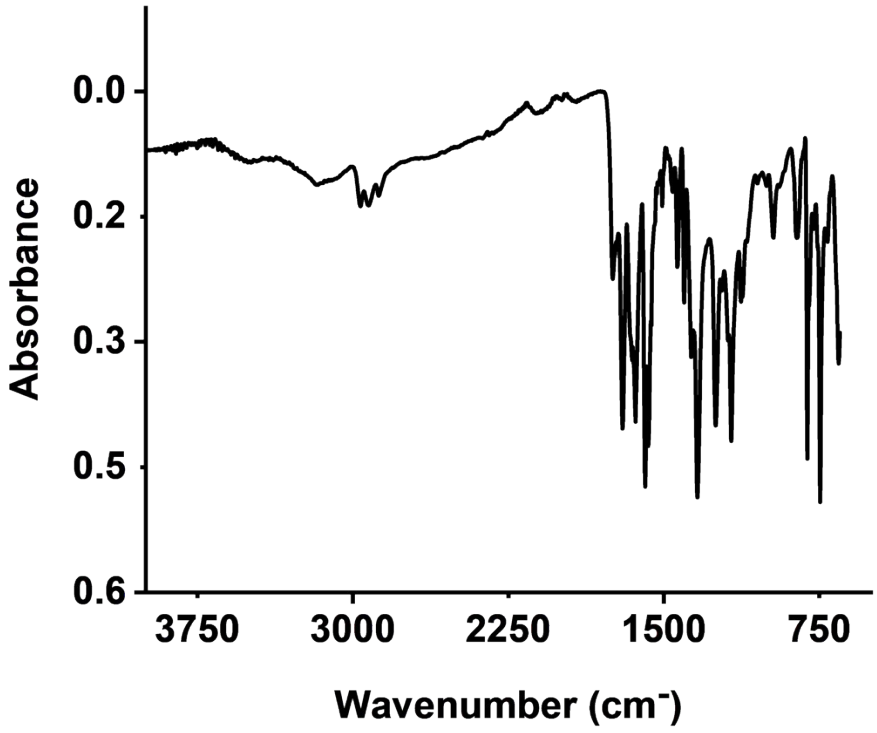

***Figure S3**. IR spectrum of **PBI-I** powder*

Analysis Info

Analysis Name	D:\Data\Mass Spectrometry Service\76146-000001.d	Acquisition Date	9/22/2020 8:40:55 AM
Method	LM MS 50 to 1100 KIM 071215.m	Operator	user
Sample Name	Dietrich-GB-PBI-I	Instrument / Ser#	micrOTOF-Q 74
Comment			

Acquisition Parameter

Source Type	ESI	Ion Polarity	Positive
Scan Begin	50 m/z		
Scan End	1100 m/z		

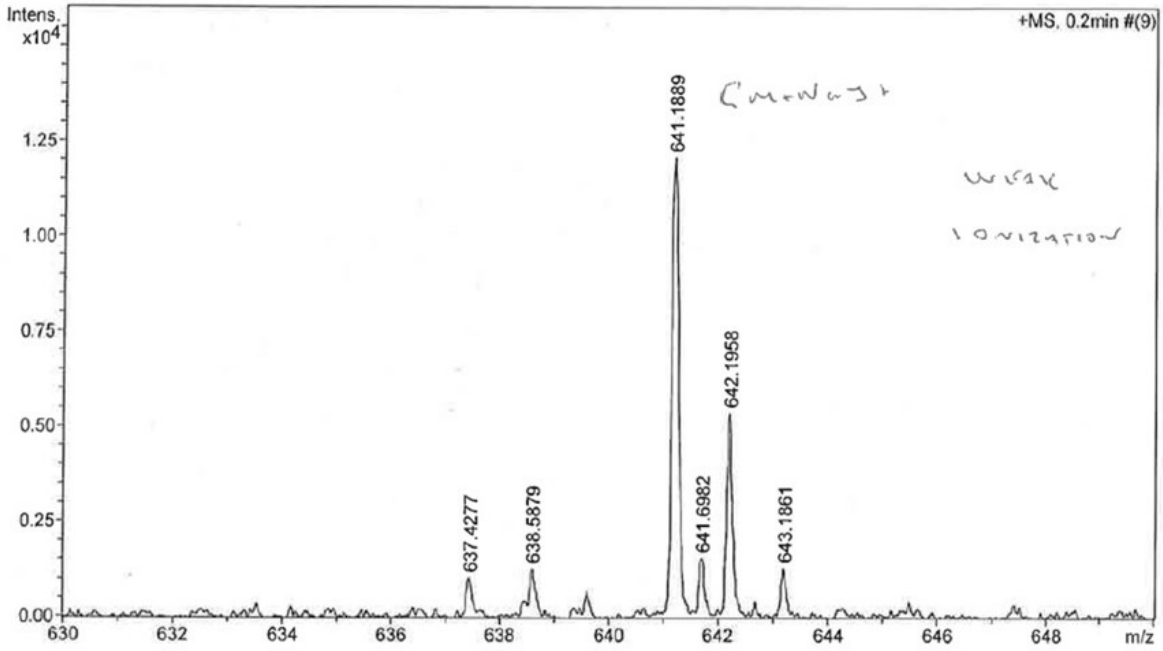

Formula	z	m/z	Meas. m/z	err [ppm]	err [mDa]
	1+		641.1889		
C 36 H 30 N 2 Na O 8		641.1894		0.9	0.6

***Figure S4**. Mass spectrum of **PBI-I** in ethanol*

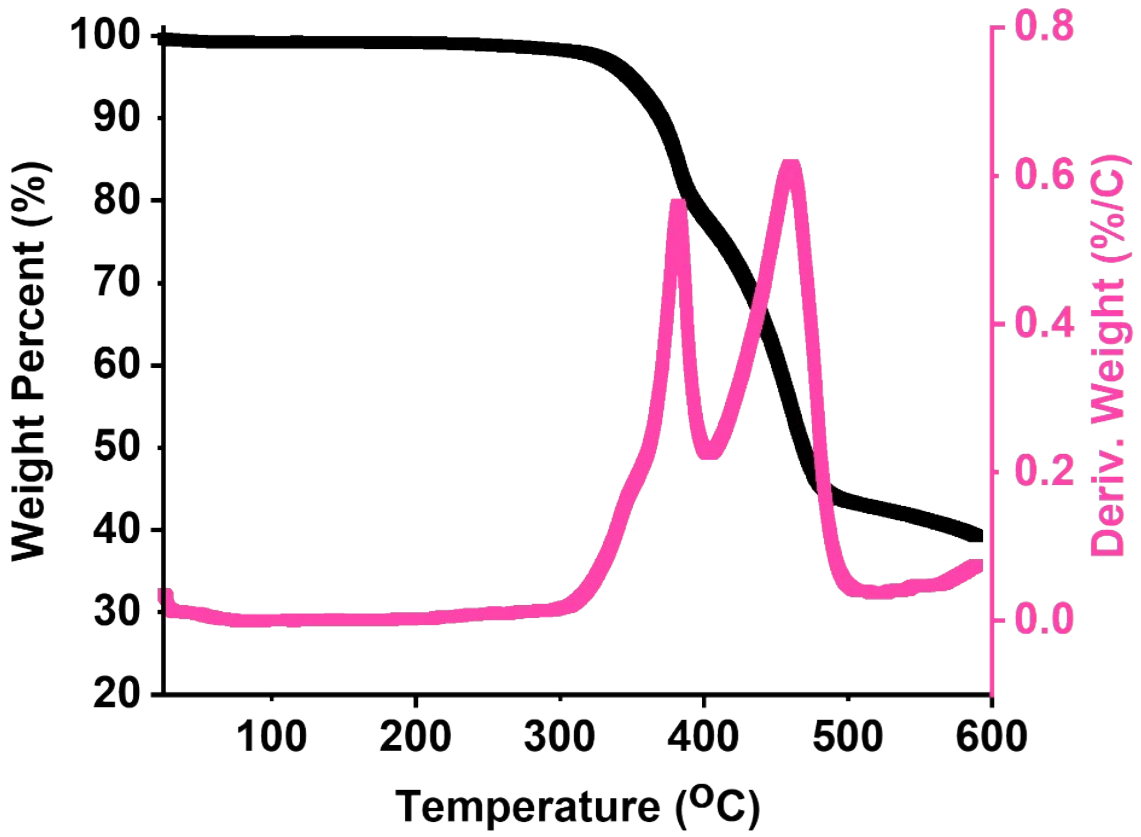

Figure S5. *Graphs showing TGA (black data) overlaid with DTG (coloured data) of* ***PBI-L*** *under* $N_2(g)$

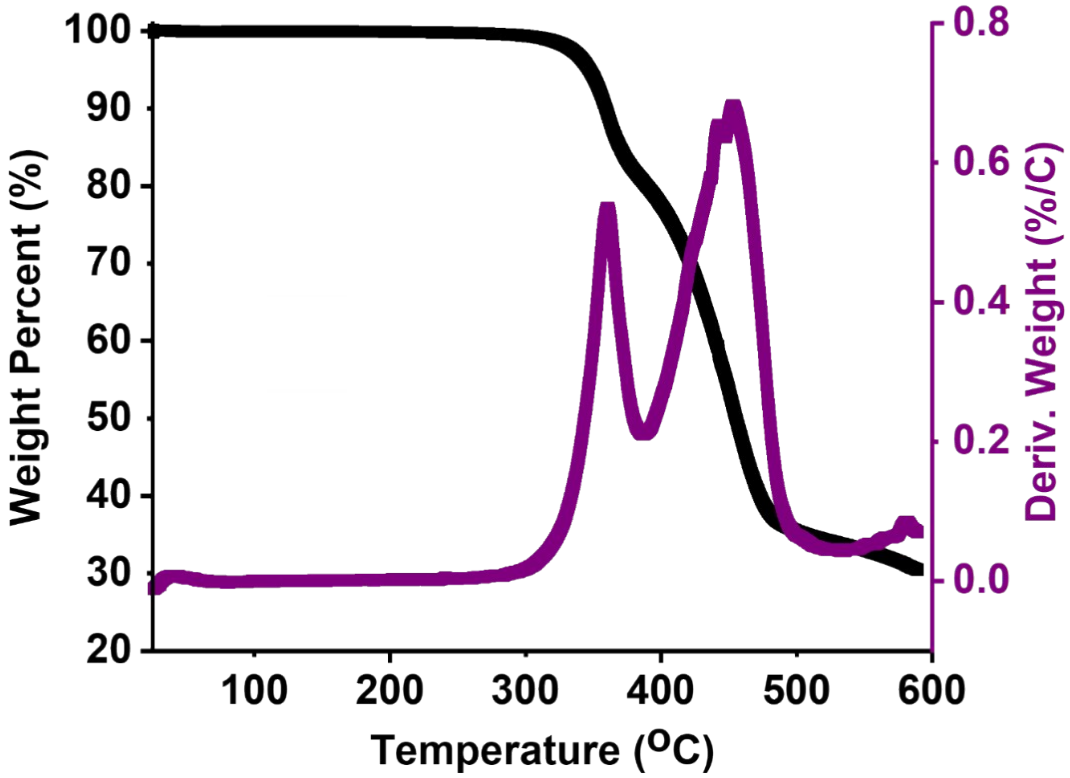

Figure S6. *Graphs showing TGA (black data) overlaid with DTG (coloured data) of* ***PBI-I*** *under* $N_2(g)$

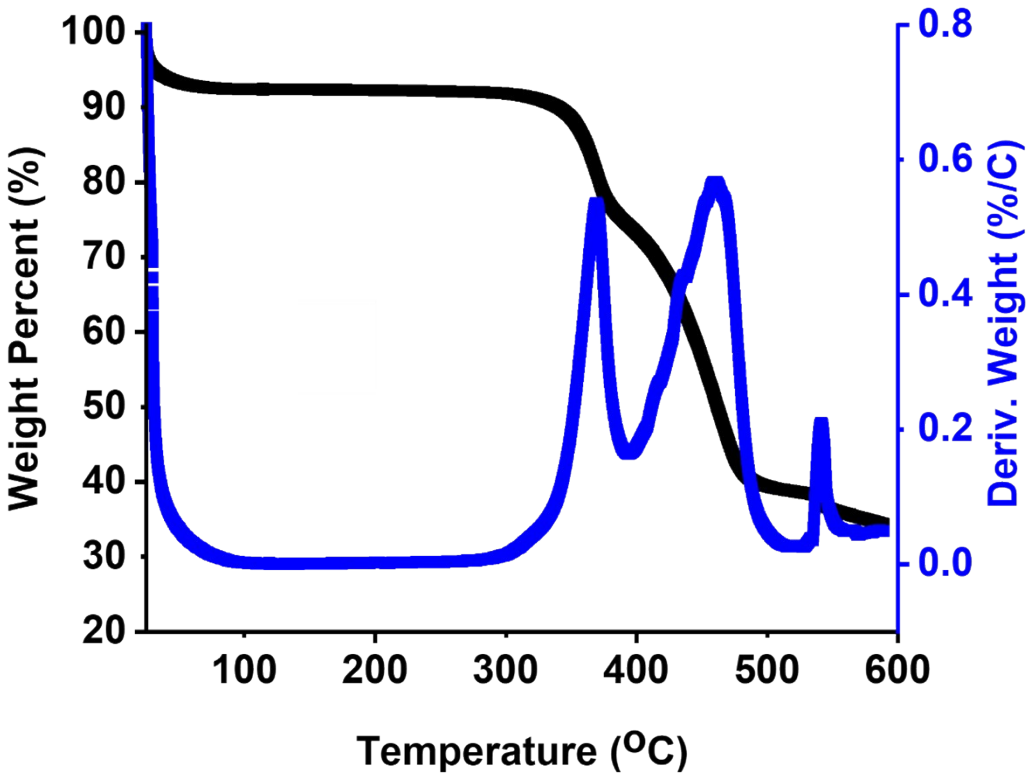

Figure S7. *Graphs showing TGA (black data) overlaid with DTG (coloured data) of* ***PBI-V*** *under N_2(g)*

3.2 Solution Characterization

Table S2. *S_0-S_1 ratio for solutions of PBIs at a concentration of 10 mg/mL and pH = 7 before and after irradiation*

PBI	S_0-S_1 ratio for solutions before irradiation	S_0-S_1 ratio for solutions after irradiation
L	0.86	0.83
I	0.85	0.84
V	0.84	0.92

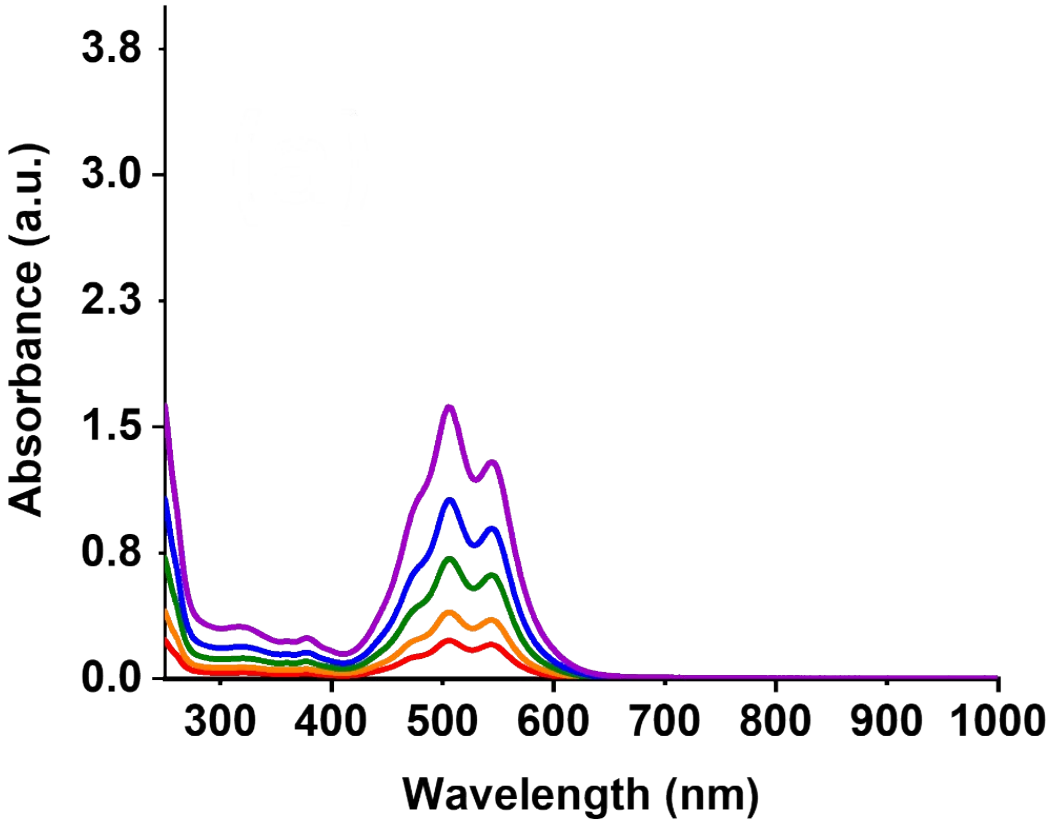

Figure S8. *UV-vis absorption spectra of* ***PBI-L*** *at pH = 7 at different concentrations. Concentration = 2.5 mg/mL (—), 5 mg/mL (—), 7.5 mg/mL (—), 10 mg/mL (—) and 15 mg/mL (—).*

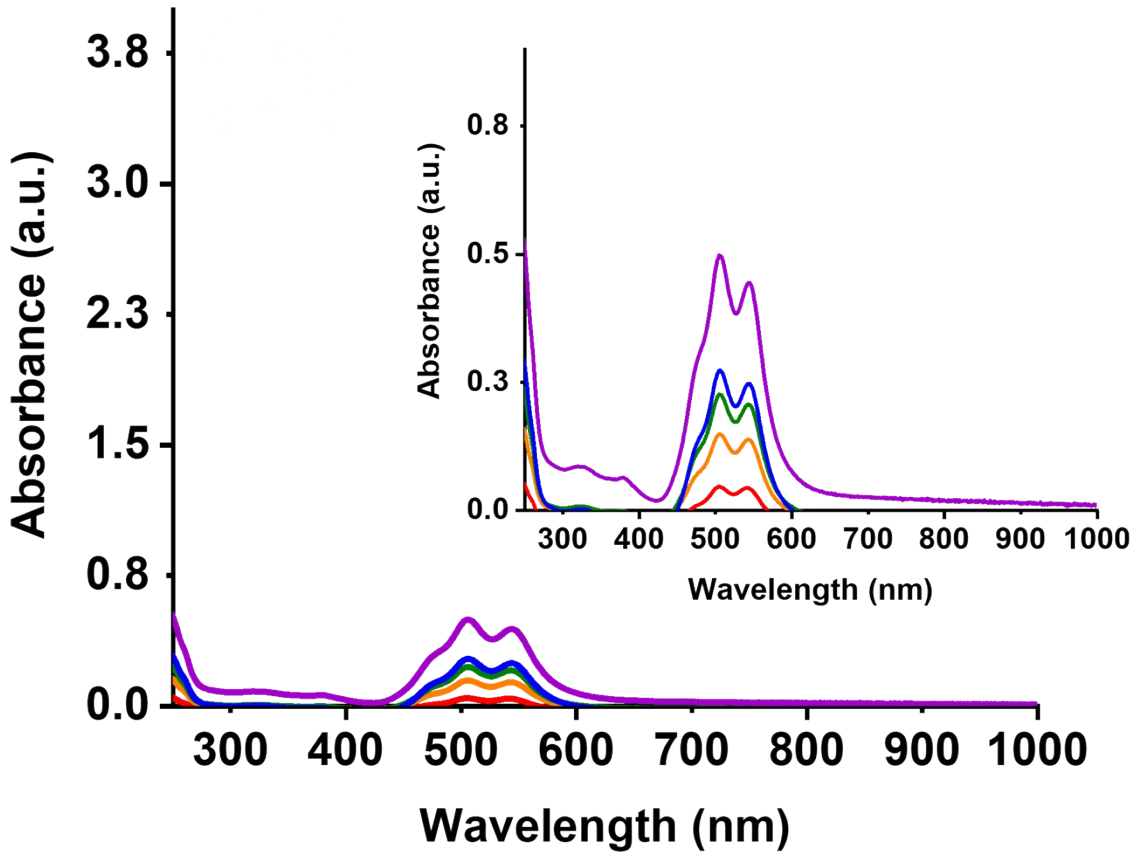

Figure S9. *UV-vis absorption spectra of* ***PBI-I*** *at pH = 7 at different concentrations, with zoomed in version. Concentration = 2.5 mg/mL (—), 5 mg/mL (—), 7.5 mg/mL (—), 10 mg/mL (—) and 15 mg/mL (—).*

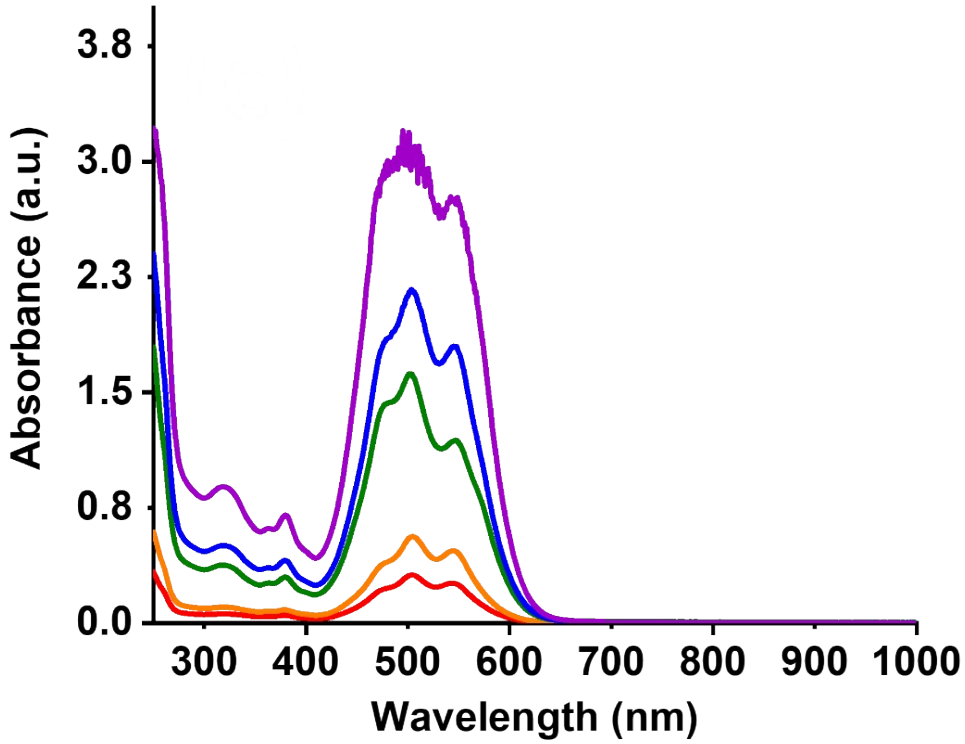

Figure S10. *UV-vis absorption spectra of* ***PBI-V*** *at pH = 7 at different concentrations. Concentration = 2.5 mg/mL (—), 5 mg/mL (—), 7.5 mg/mL (—), 10 mg/mL (—) and 15 mg/mL (—).*

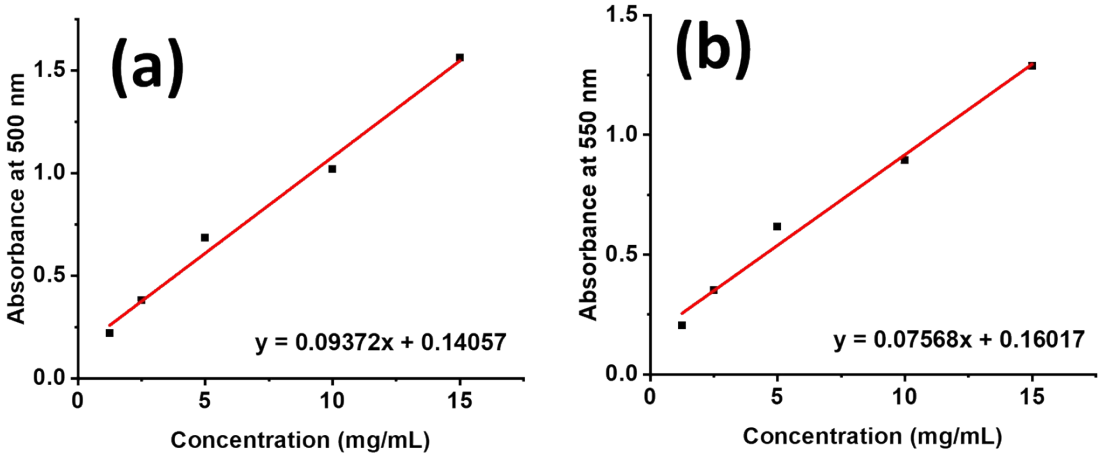

Figure S11. *The molar absorptivity for* ***PBI-L*** *for the absorbance peak at (a) 500 nm and is absorbance peaks at (b) 550 nm; stock solutions were measured in a 10 mm quartz cuvette.*

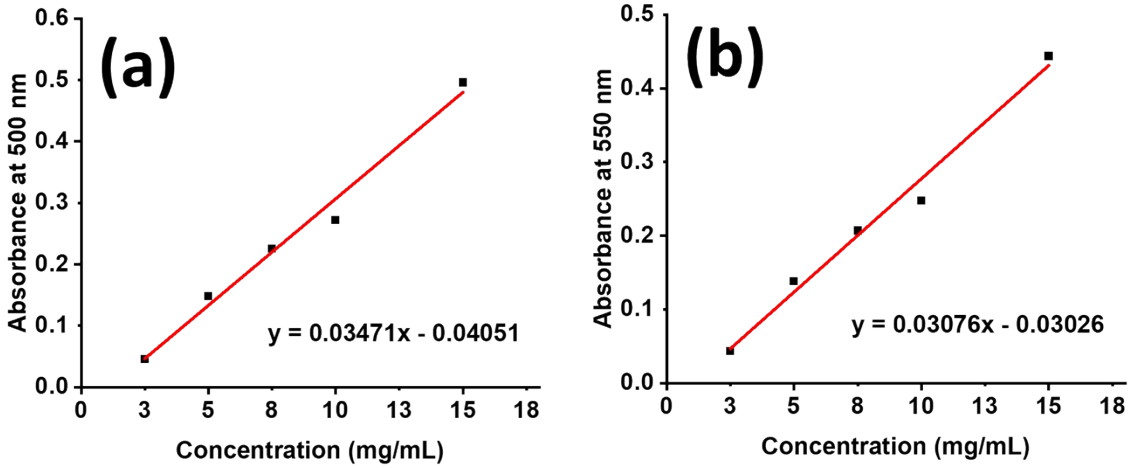

Figure S12. *The molar absorptivity for* ***PBI-I*** *for the absorbance peak at (a) 500 nm and is absorbance peaks at (b) 550 nm; stock solutions were measured in a 10 mm quartz cuvette.*

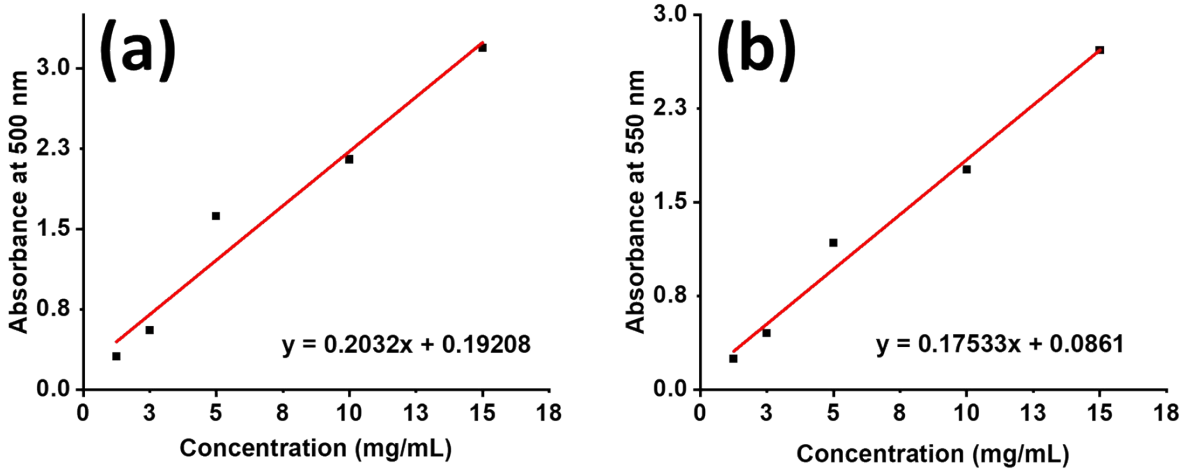

Figure S13. *The molar absorptivity for* ***PBI-V*** *for the absorbance peak at (a) 500 nm and is absorbance peaks at (b) 550 nm; stock solutions were measured in a 10 mm quartz cuvette.*

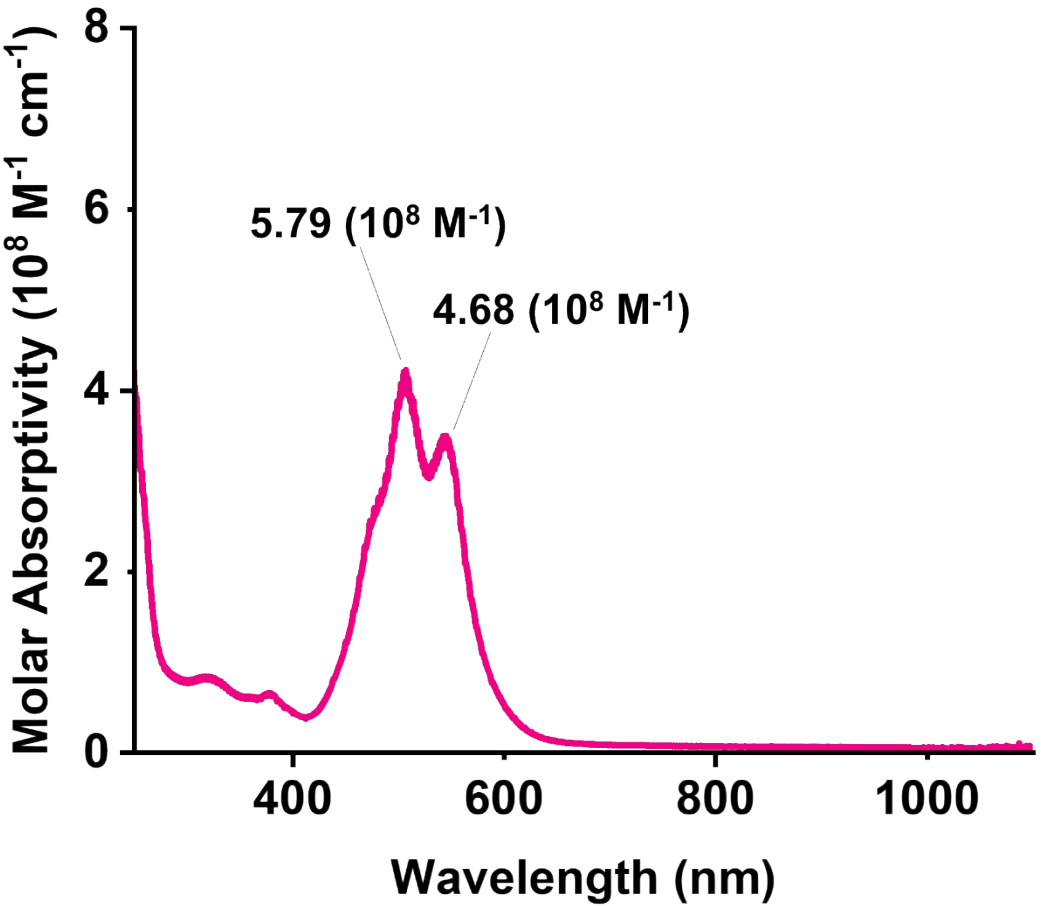

Figure S14. *Molar absorptivity spectra* ***PBI-L****.*

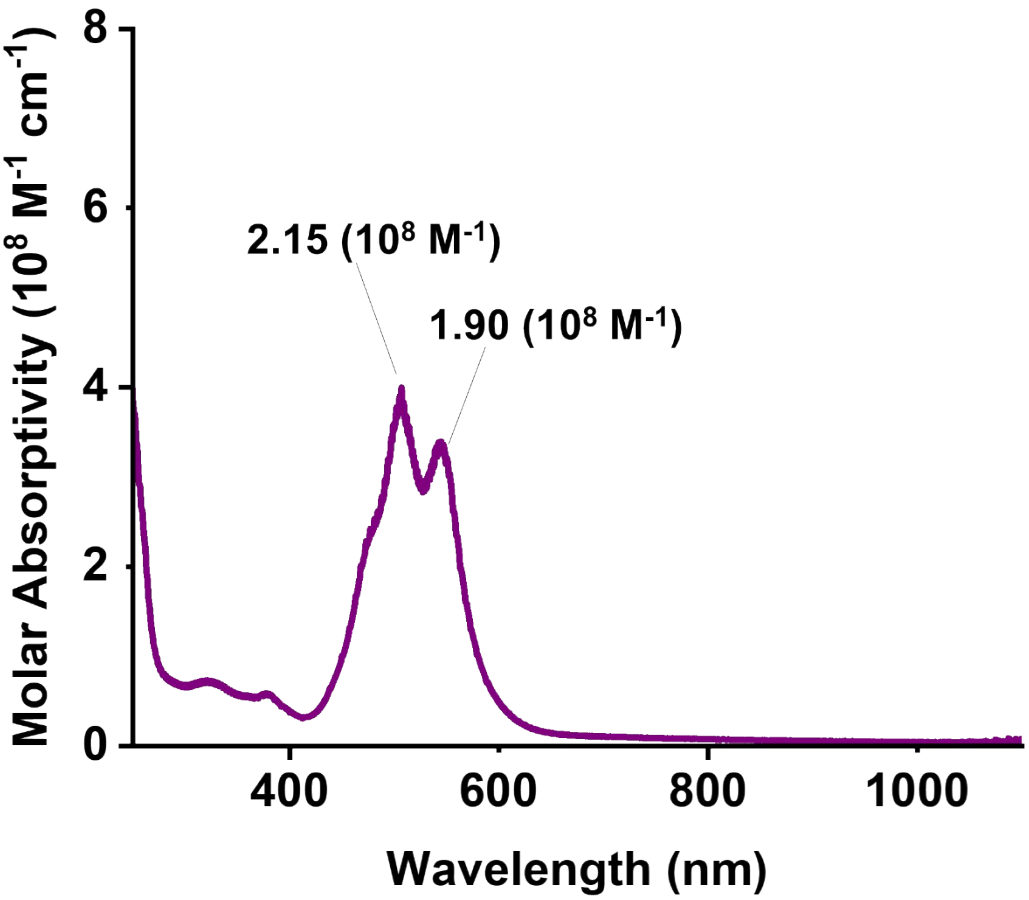

Figure S15. *Molar absorptivity spectra of* ***PBI-I****.*

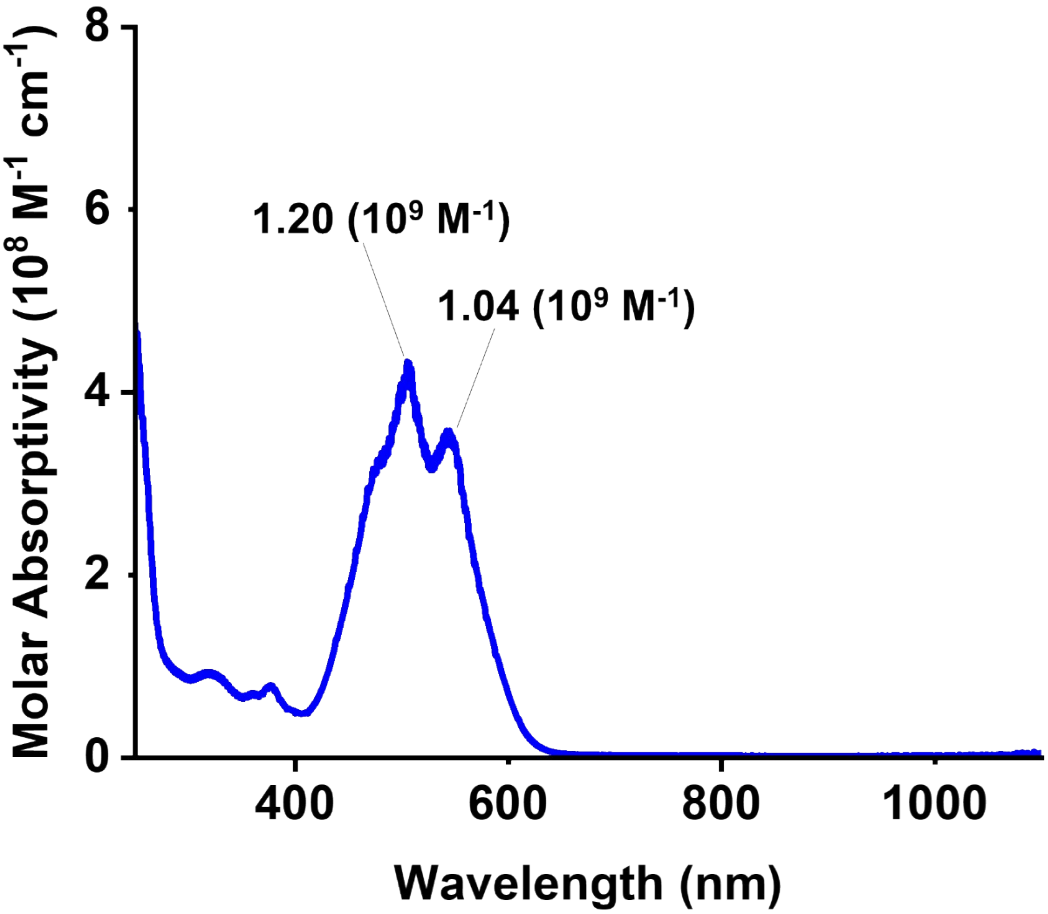

Figure S16. *Molar absorptivity spectra* ***PBI-V****.*

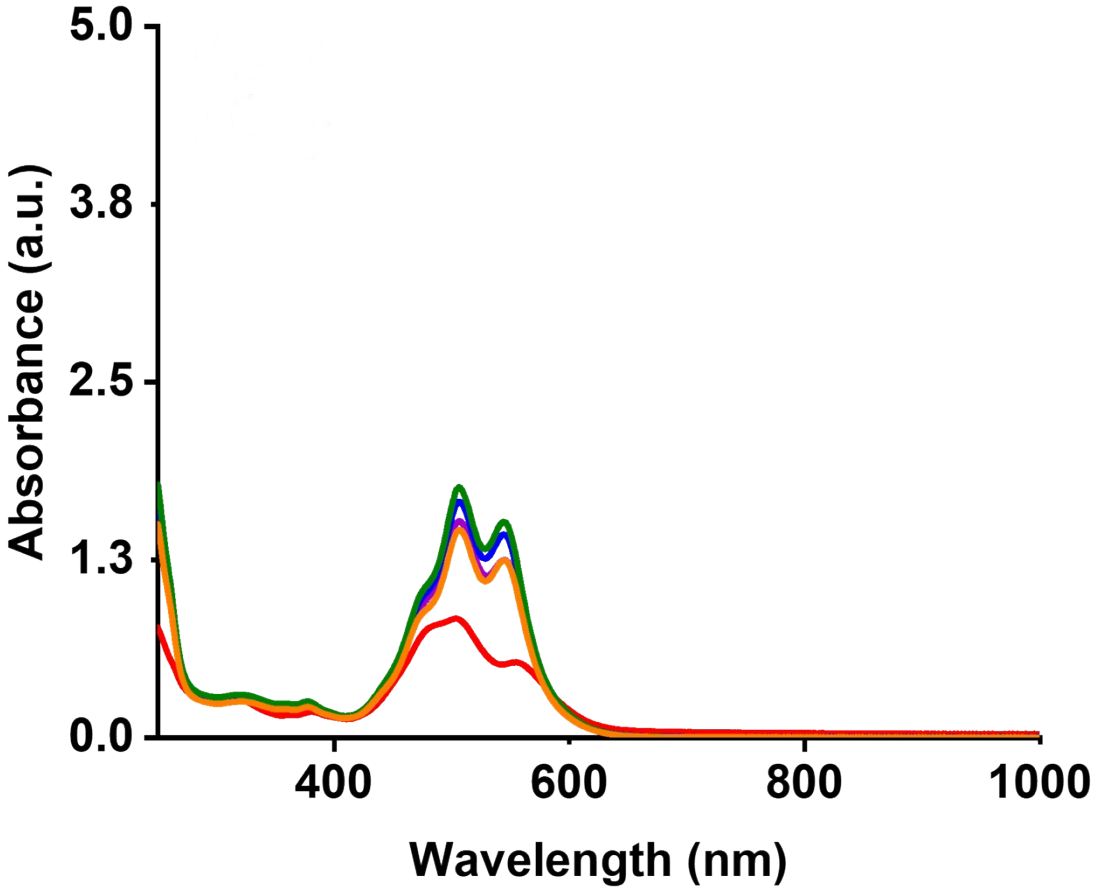

Figure S17. *UV-vis absorption spectra of* ***PBI-L****. UV-vis absorption spectroscopy measurements were done at pH = 5 (—), pH = 6 (—), pH = 7 (—), pH = 8 (—), and pH = 9 (—).*

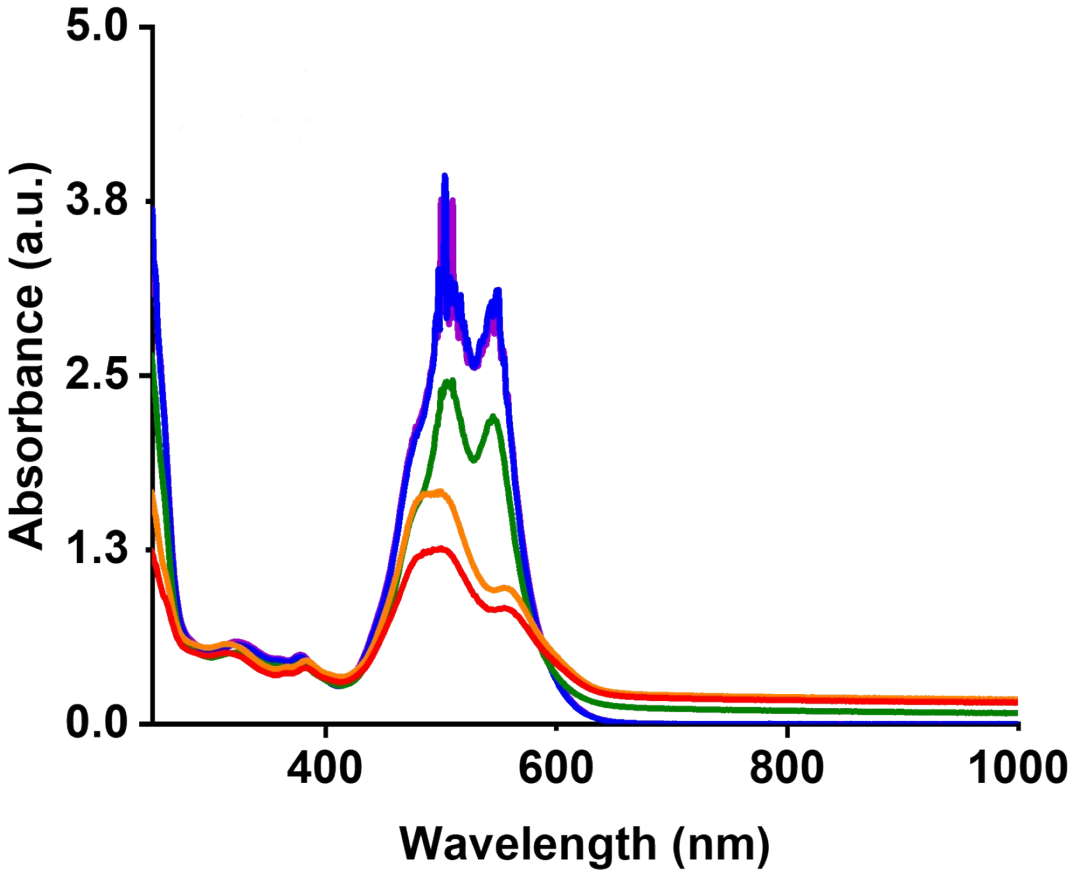

Figure S18. *UV-vis absorption spectra of* ***PBI-I****. UV-vis absorption spectroscopy measurements were done at pH = 5 (—), pH = 6 (—), pH = 7 (—), pH = 8 (—), and pH = 9 (—).*

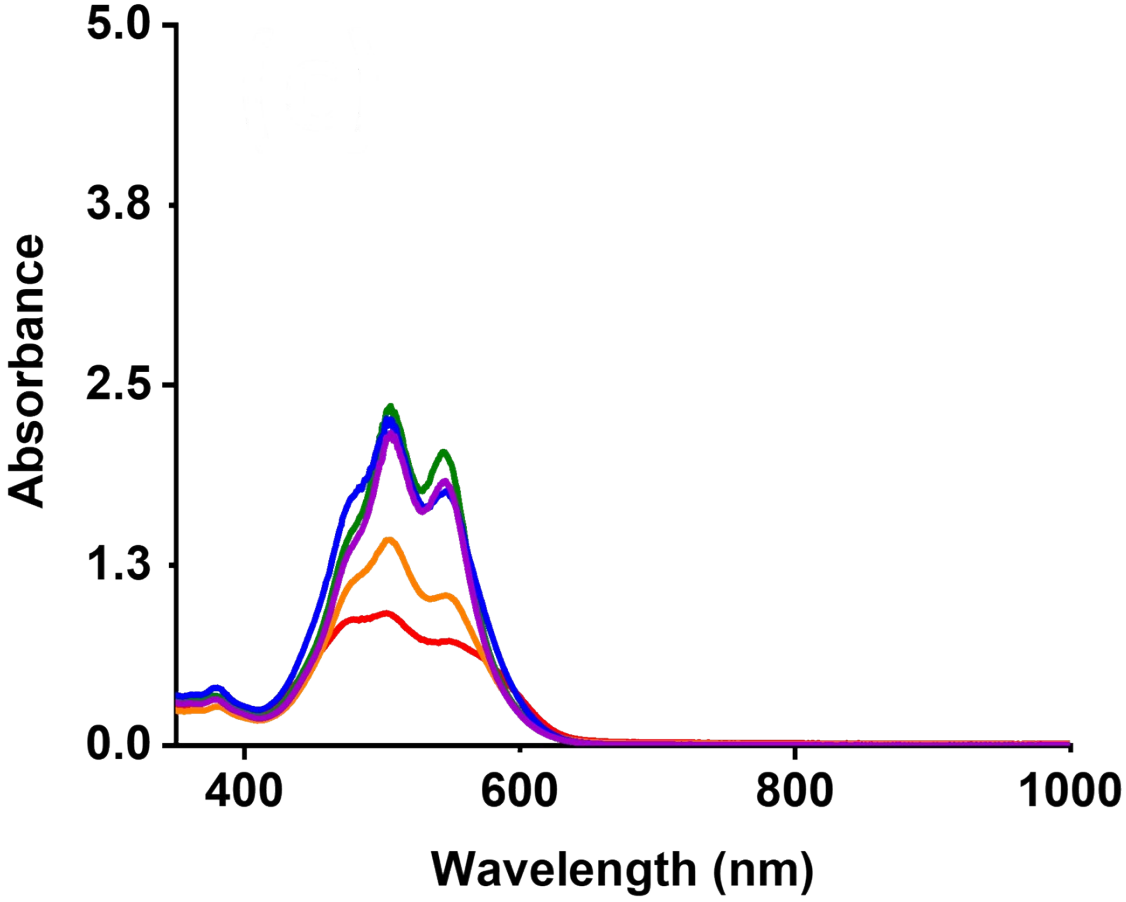

Figure S19. *UV-vis absorption spectra of* ***PBI-V****. UV-vis absorption spectroscopy measurements were done at pH = 5 (—), pH = 6 (—), pH = 7 (—), pH = 8 (—), and pH = 9 (—).*

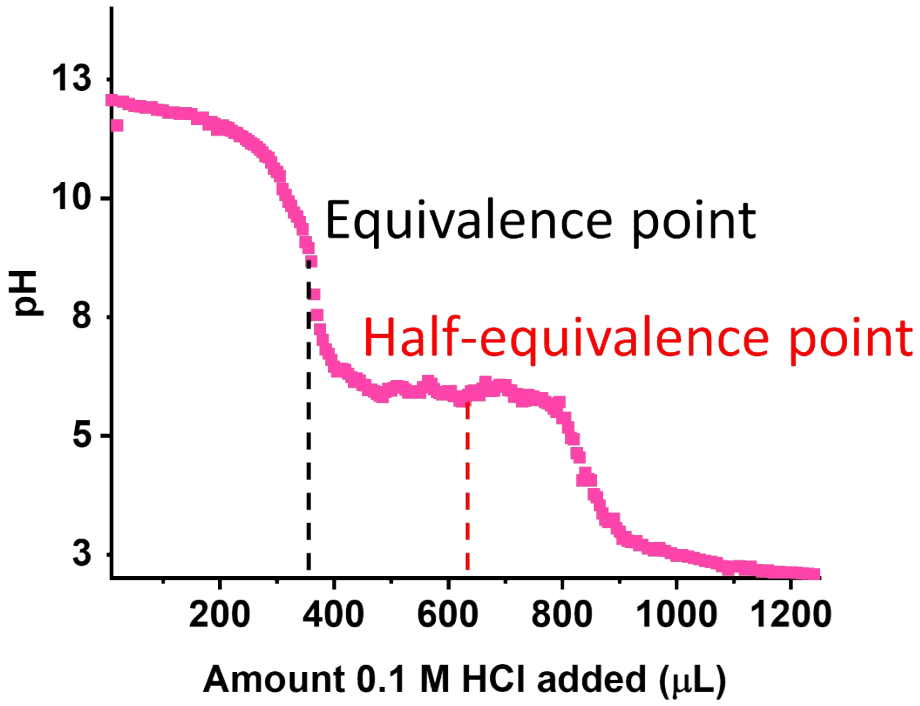

Figure S20. *Apparent pK_a 'titration' for a 10 mg/mL solution of* ***PBI-L*** *(—) using 0.1 M HCl solution.*

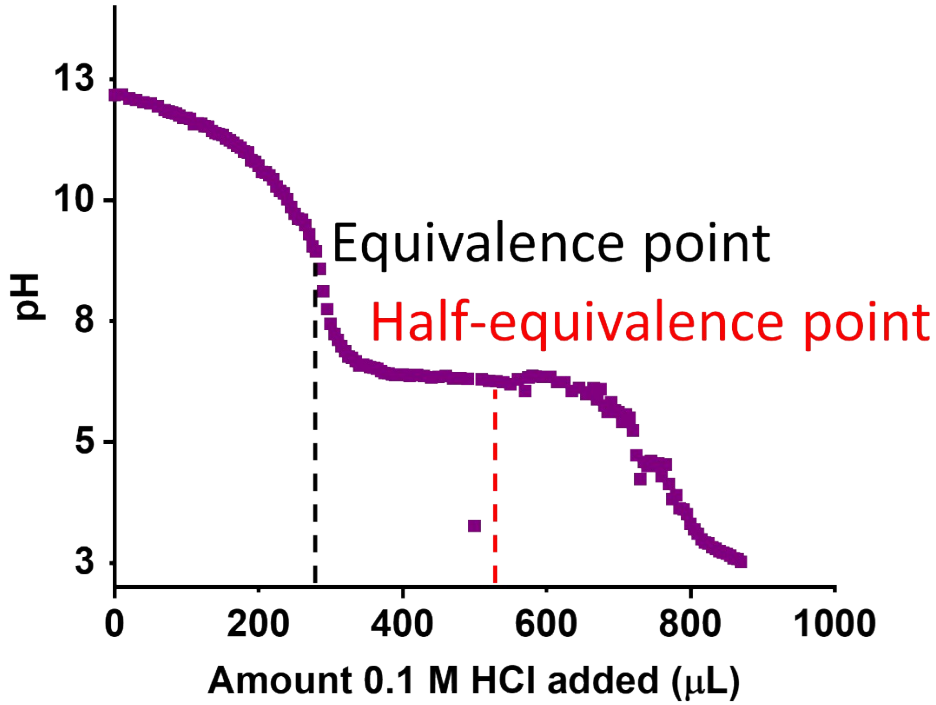

Figure S21. *Apparent pK_a 'titration' for a 10 mg/mL solution of* ***PBI-I*** *(—) using 0.1 M HCl solution.*

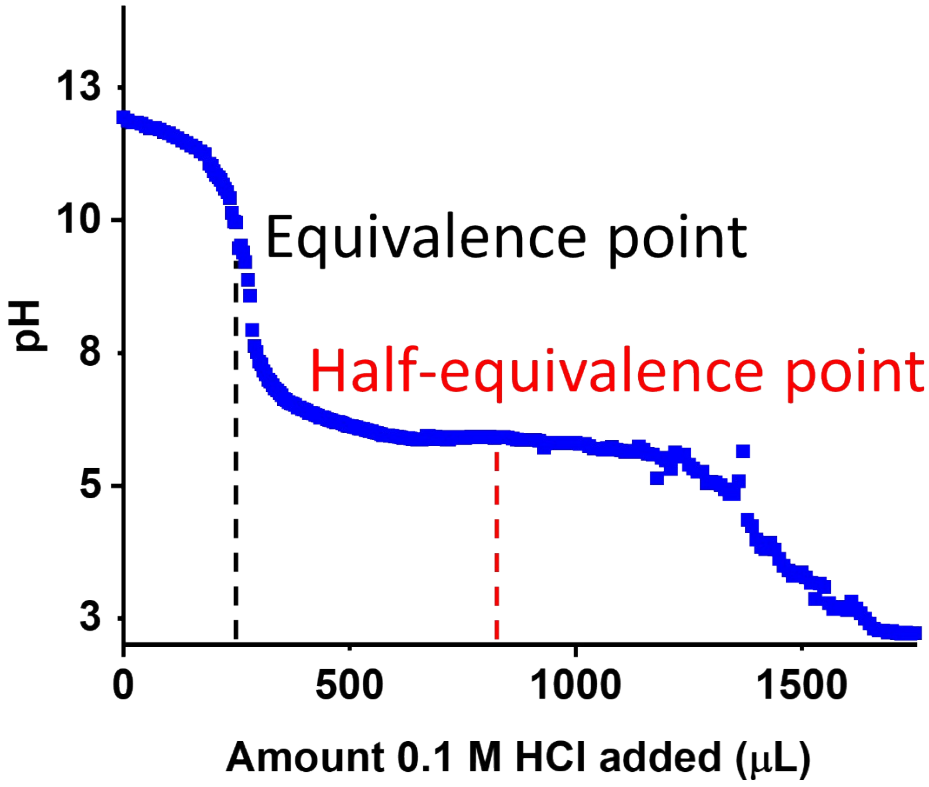

Figure S22. *Apparent pK_a 'titration' for a 10 mg/mL solution of* ***PBI-V*** *(—) using 0.1 M HCl solution.*

Table S3. *Apparent pK_a of the PBIs as determine from the pK_a titration.*

PBI	**L**	**I**	**V**
pK_a	5.98	6.31	5.90
Moles of HCl added for pK_a (mol)	$6.1 \cdot 10^{-5}$	$4.7 \cdot 10^{-5}$	$8.6 \cdot 10^{-5}$

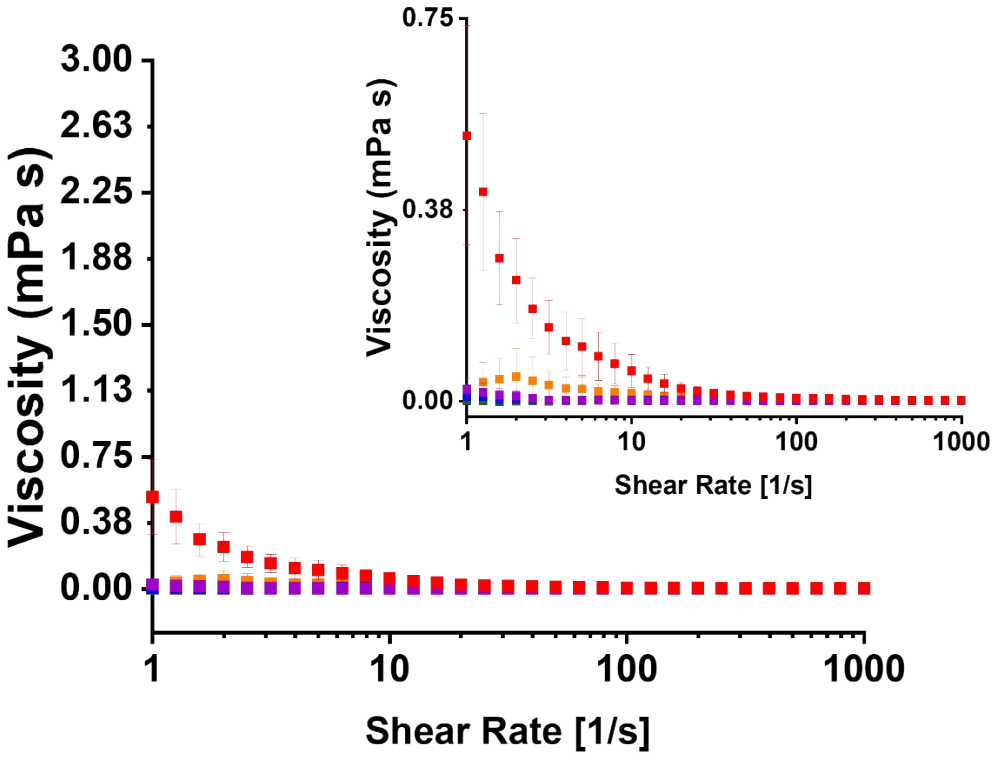

***Figure S23**. Dynamic viscosity of **PBI-L** on comparable axis and with zoomed in plots. Viscosity measurements were done at pH = 5 (—), pH = 6 (—), pH = 7 (—), pH = 8 (—), and pH = 9 (—). Measurements were performed in triplicate and errors were calculated from the standard deviation.*

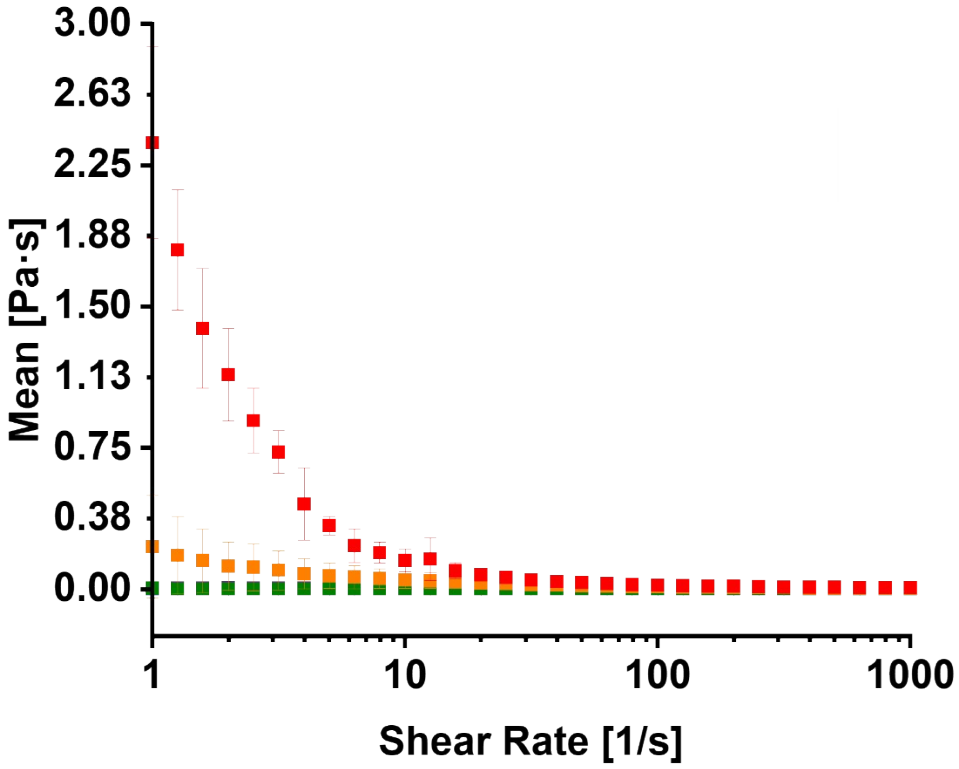

***Figure S24**. Dynamic viscosity of **PBI-I** on comparable axis. Viscosity measurements were done at pH = 5 (—), pH = 6 (—), pH = 7 (—), pH = 8 (—), and pH = 9 (—). Measurements were performed in triplicate and errors were calculated from the standard deviation.*

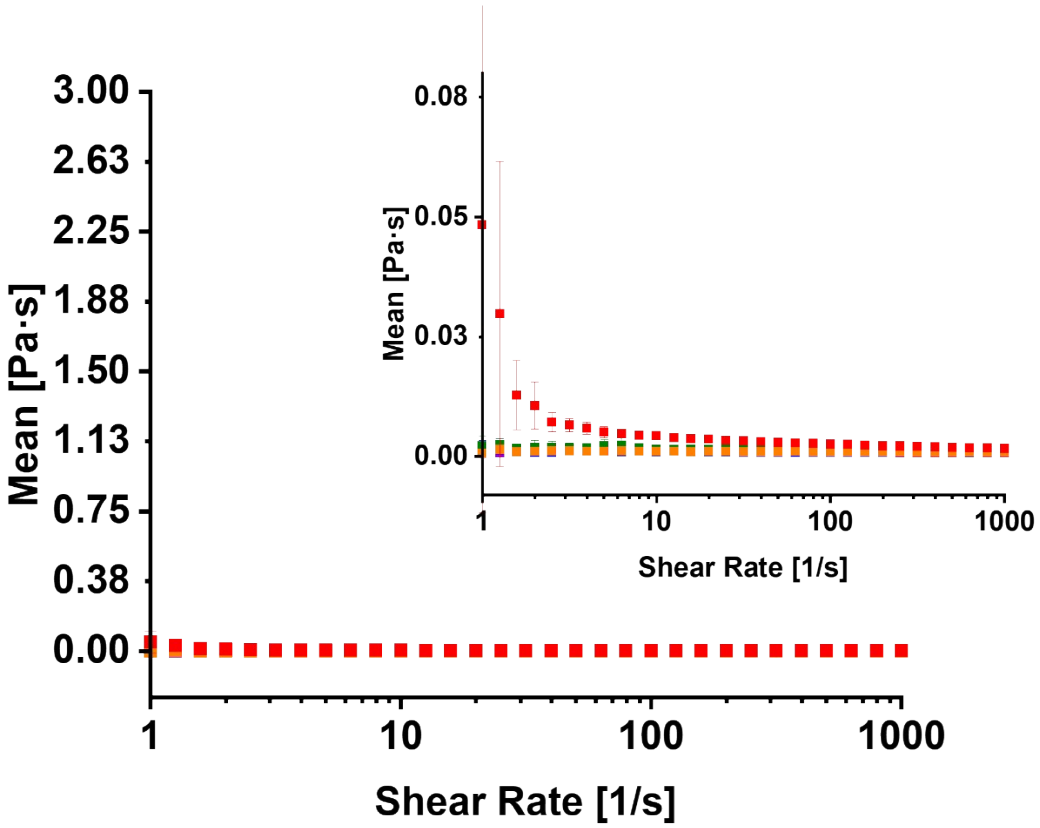

***Figure S25**. Dynamic viscosity of **PBI-V** on comparable axis and with zoomed in plots. Viscosity measurements were done at pH = 5 (—), pH = 6 (—), pH = 7 (—), pH = 8 (—), and pH = 9 (—). Measurements were performed in triplicate and errors were calculated from the standard deviation.*

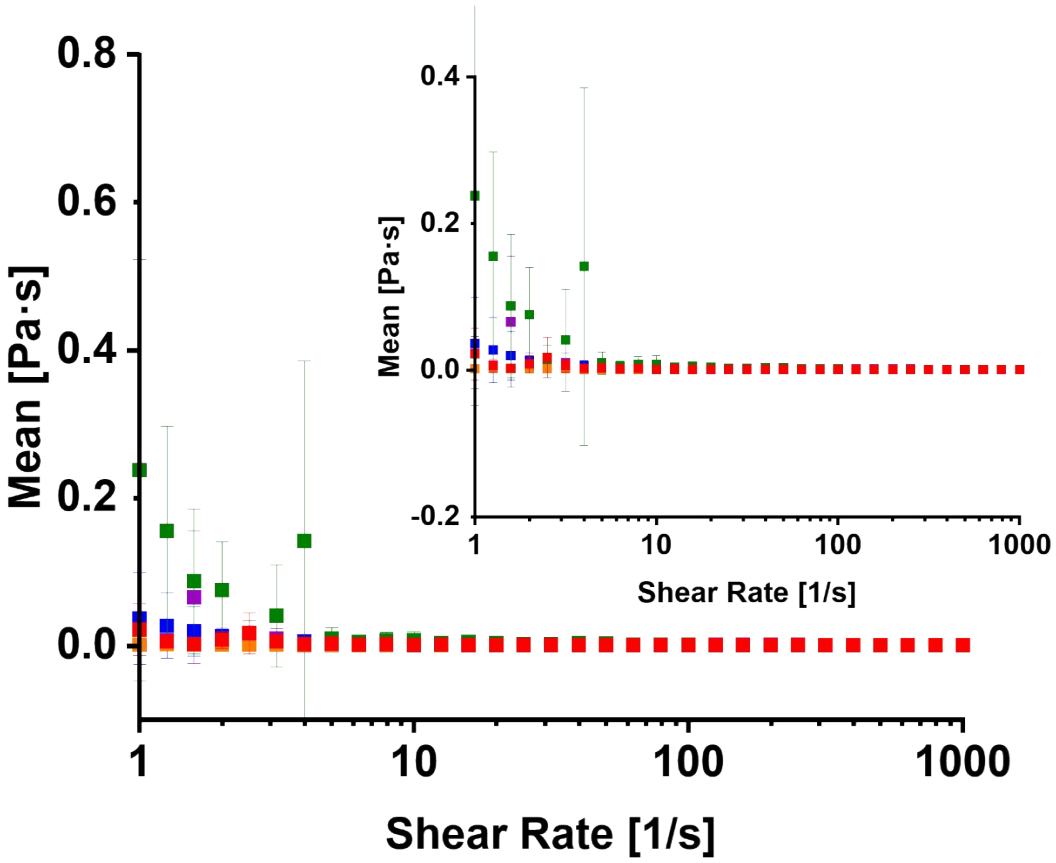

***Figure S26**. Dynamic viscosity measurements **PBI-L** at pH = 7 at different concentrations on comparable axis as well as zoomed in plots. Concentrations = 2.5 mg/mL (—), 5 mg/mL (—), 7.5 mg/mL (—), 10 mg/mL (—) and 15 mg/mL (—). Measurements were performed in triplicate and errors were calculated from the standard deviation.*

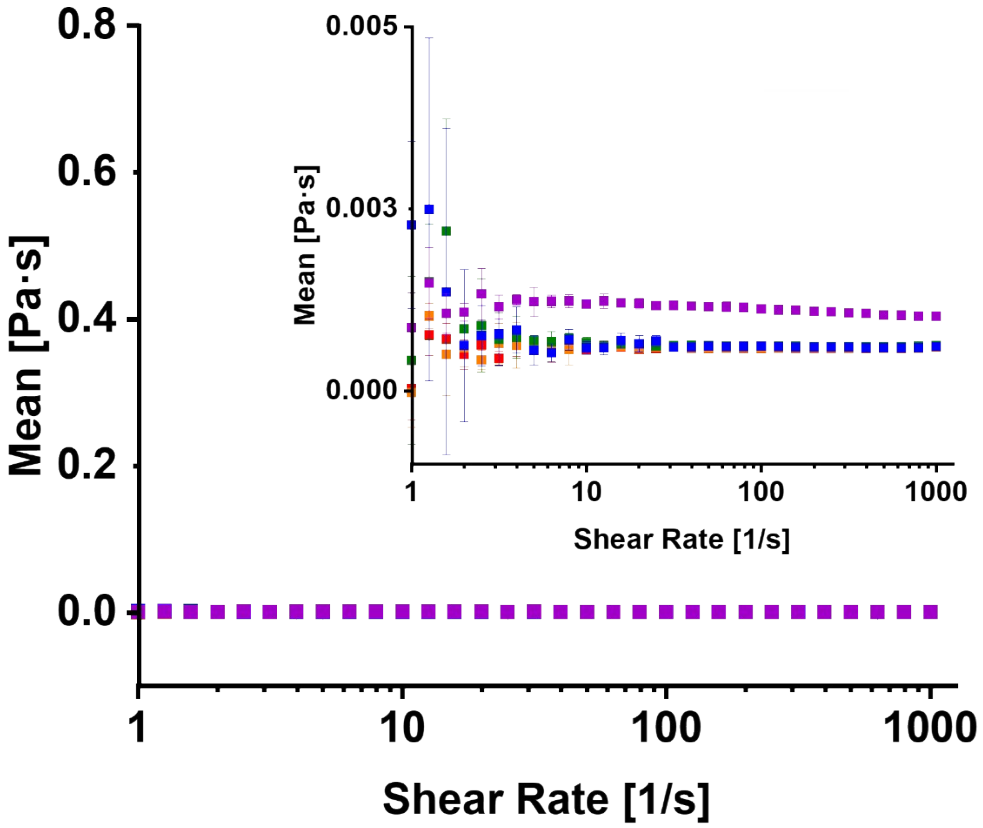

Figure S27. *Dynamic viscosity measurements* ***PBI-I*** *at pH = 7 at different concentrations on comparable axis as well as zoomed in plots. Concentrations = 2.5 mg/mL (—), 5 mg/mL (—), 7.5 mg/mL (—), 10 mg/mL (—) and 15 mg/mL (—). Measurements were performed in triplicate and errors were calculated from the standard deviation.*

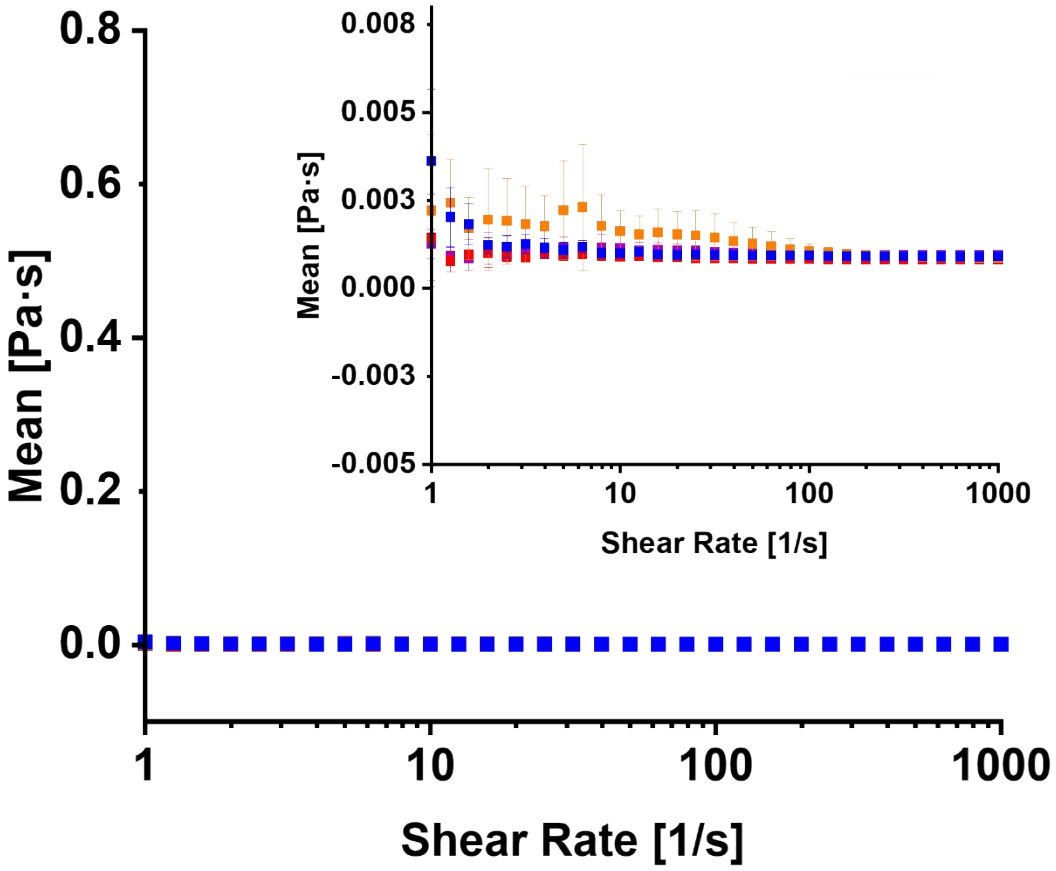

Figure S28. *Dynamic viscosity measurements (c)* ***PBI-V*** *at pH = 7 at different concentrations on comparable axis as well as zoomed in plots. Concentrations = 2.5 mg/mL (—), 5 mg/mL (—), 7.5 mg/mL (—), 10 mg/mL (—) and 15 mg/mL (—). Measurements were performed in triplicate and errors were calculated from the standard deviation.*

Table S4. *SAXS fitting results for* ***PBI-L*** *as 10 mg/mL solutions at different pH. *No fitting error available.*

pH	*Model*	*Length / nm*	*Kuhn Length / nm*	*Cylinder Radius / nm*	*Axis Ratio*	*Sphere radius / nm*	*Power law*	X^2
3	Flexible elliptical cylinder + power	3000*	4.74 ± 0.0268	1.44 ± 0.00577	2.16 ± 0.0104	**N/A**	4.22 0.00296	2.6
7	Half Sphere	**N/A**	**N/A**	**N/A**	**N/A**	1.18 ± 0.00351	**N/A**	1.6
7	Half Power	**N/A**	**N/A**	**N/A**	**N/A**	**N/A**	3.46 ± 0.00011	13

Table S5. *SAXS fitting results for* ***PBI-I*** *as 10 mg/mL solutions at different pH. *No fitting error available.*

pH	*Model*	*Length / nm*	*Kuhn Length / nm*	*Cylinder Radius / nm*	*Axis Ratio*	*Sphere radius / nm*	*Power law*	X^2
3	Flexible elliptical cylinder + power	1380 ± 38.1	7.55 ± 0.0217	1.37 ± 0.00219	2.81 ± 0.00766	**N/A**	6.02 ± 0.0325	1.7
6	Flexible elliptical cylinder + power	20.6 ± 0.463	22.4 ± 0.371	1.52 ± 0.000512	2.17 ± 0.0157	**N/A**	2.22 ± 0.000158	1.7
7	Sphere + Power	**N/A**	**N/A**	**N/A**	**N/A**	1.16 ± 0.00383	2.48 ± 0.000881	7.1

Table S6. *SAXS fitting results for* ***PBI-V*** *as 10 mg/mL solutions at different pH. *No fitting error available.*

pH	*Model*	*Length / nm*	*Kuhn Length / nm*	*Cylinder Radius / nm*	*Axis Ratio*	*Sphere radius / nm*	*Power law*	X^2
3	Flexible elliptical cylinder + power	3000*	0.631 ± 0.144	1.81 ± 0.00612	4.18 ± 0.00133	**N/A**	3.01 ± 0.0197	9.4
5	Flexible elliptical cylinder + sphere	3000*	0.217 ± 0.000416	1.63 ± 0.000784	4.09 ± 0.00349	4.85 ± 0.00331	**N/A**	11
6	Flexible elliptical cylinder + sphere	3000*	0.265 ± 0.00169	1.57 ± 0.00139	4.55 ± 0.00525	4.13 ± 0.00298	**N/A**	10
7	Sphere + Power	**N/A**	**N/A**	**N/A**	**N/A**	3.83 0.00782	1.43 0.00217	2.1

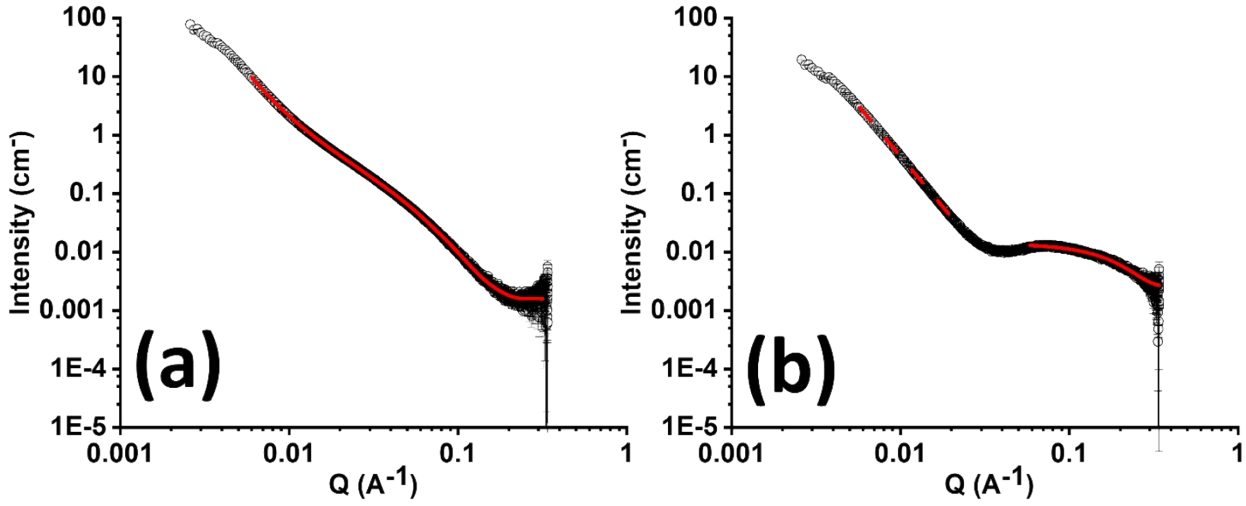

Figure S29. *SAXS data for* ***PBI-L*** *at different pHs showing scattering vector vs scattering intensity (open black circles) with the corresponding model fits (solid red lines). (a) pH = 3 (b) pH = 7*

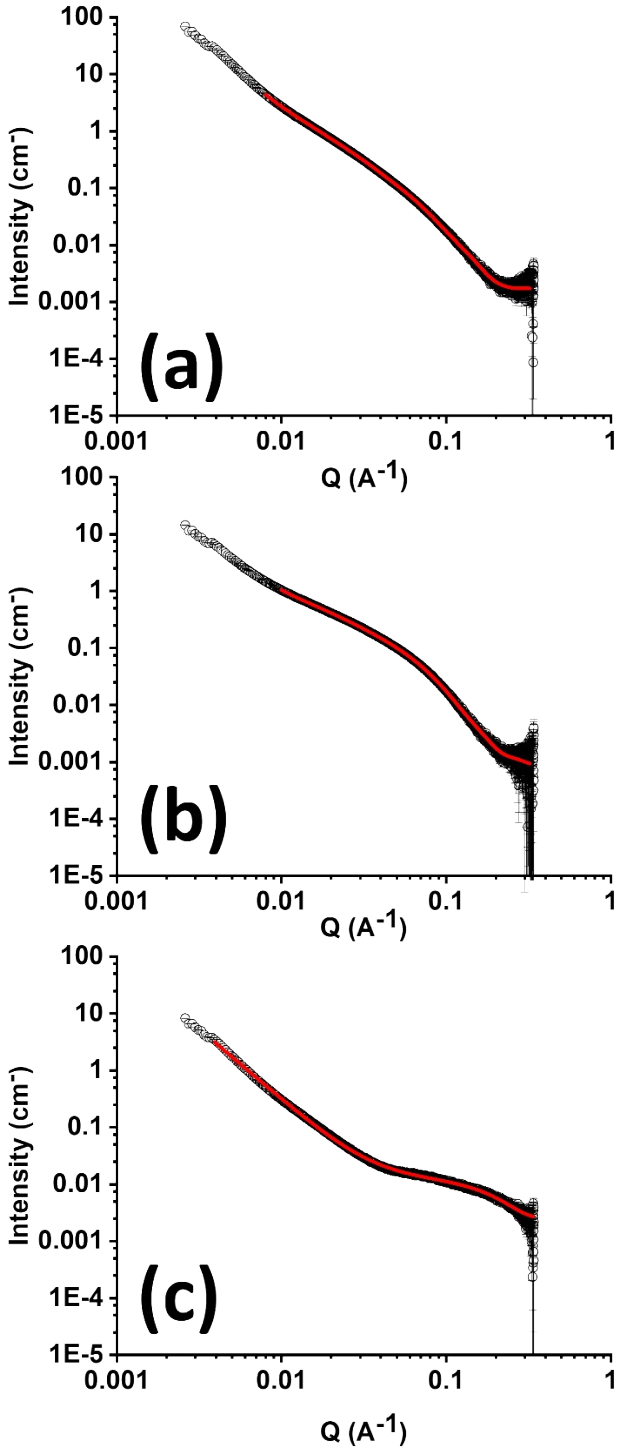

Figure S30. *SAXS data for* ***PBI-I*** *at different pHs showing scattering vector vs scattering intensity (open black circles) with the corresponding model fits (solid red lines). (a) pH = 3 (b) pH = 6 (c) pH = 7*

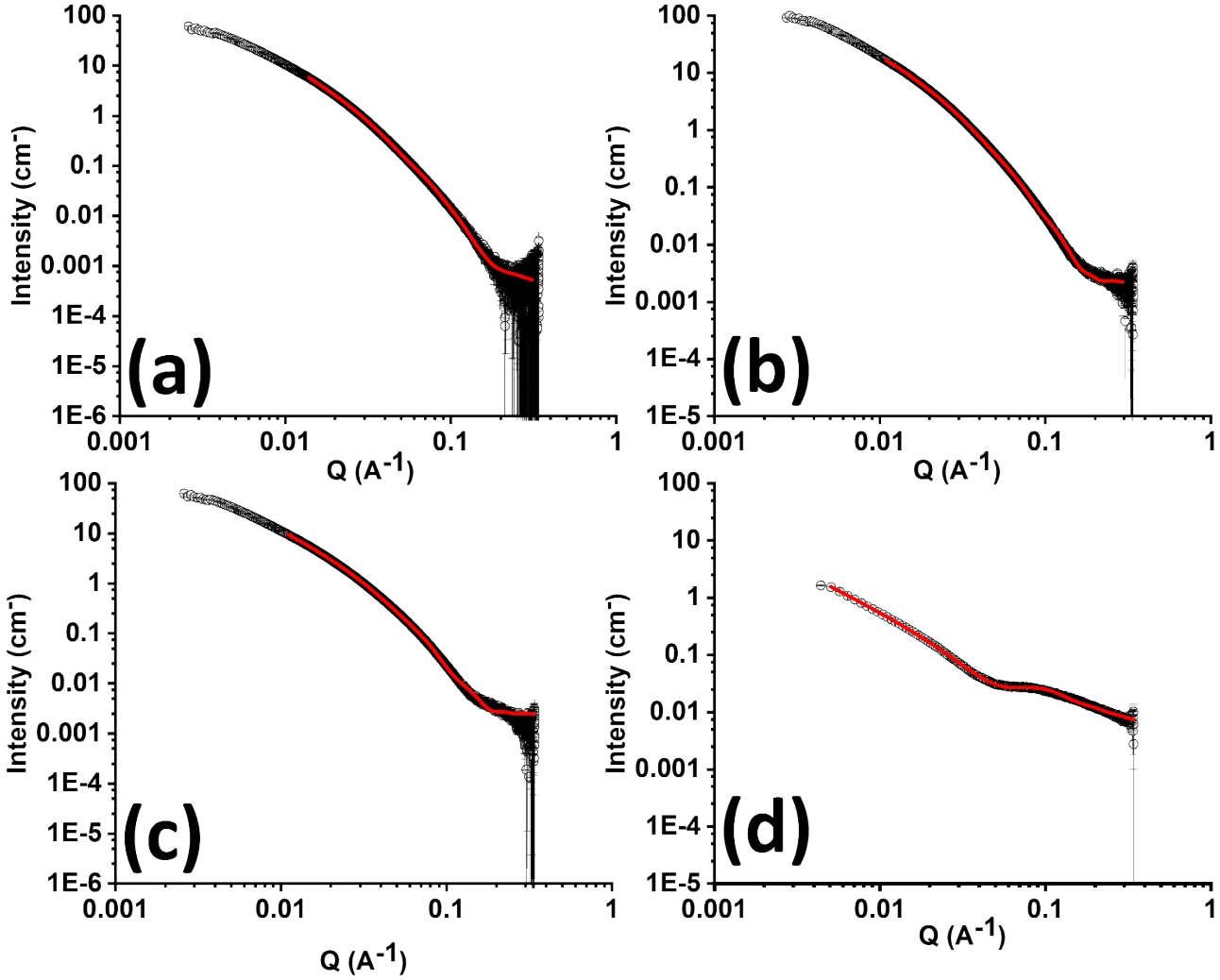

Figure S31. *SAXS data for* ***PBI-V*** *at different pHs showing scattering vector vs scattering intensity (open black circles) with the corresponding model fits (solid red lines). (a) pH = 3 (b) pH = 5 (c) pH = 6 (d) pH = 7*

Table S7. *SAXS fitting attempts for* ***PBI-L*** *as 10 mg/mL solutions pH = 5. *No fitting error available.*

Model	*Length / nm*	*Kuhn Length / nm*	*Cylinder Radius / nm*	*Axis Ratio*	*Sphere radius / nm*	*Power law*	X^2
Flexible elliptical cylinder	3000*	23.1 ± 0.0321	1.16 ± 0.00152	9.03 ± 0.0129	**N/A**	**N/A**	2297
Flexible elliptical cylinder + power	74.9 ± 0.351	18.7 ± 0.0000127	1.38 ± 0.00151	3.71 ± 0.00523	**N/A**	3.86 0.00361	75
Flexible elliptical cylinder + sphere	3000*	24.3 ± 0.0242	2.31 ± 0.00167	2.73 ± 0.00467	6.78 ± 0.00411	**N/A**	1875
Flexible cylinder polydisperse 0.3	3000*	7.07 ± 0.0147	2.61 ± 0.00148	**N/A**	**N/A**	**N/A**	3250
Flexible cylinder polydisperse 0.3 + power	3000*	4.61 ± 0.0141	1.85 ± 0.00141	**N/A**	**N/A**	4.66 ± 0.00201	102
Flexible cylinder polydisperse 0.3 + sphere	3000*	5.39 ± 0.0217	1.98 ± 0.00201	**N/A**	3.54 ± 0.0396	**N/A**	62

Table S8. *SAXS fitting attempts for* ***PBI-L*** *as 10 mg/mL solutions pH = 6. *No fitting error available.*

Model	*Length / nm*	*Kuhn Length / nm*	*Cylinder Radius / nm*	*Axis Ratio*	*Sphere radius / nm*	*Power law*	X^2
Flexible elliptical cylinder	3000*	25*	0.393 ± 0.00256	1560 ± 7.41	**N/A**	**N/A**	194
Flexible elliptical cylinder + power	3000*	25*	0.293 ± 0.00224	314 ± 2.78	**N/A**	3.25 ± 0.0210	15
Flexible elliptical cylinder + sphere	3000*	25*	0.633 ± 0.0373	113 ± 6.89	3.57 ± 0.00521	**N/A**	49
Flexible cylinder polydisperse 0.15	3000*	20*	3.35 ± 0.00183	**N/A**	**N/A**	**N/A**	373
Flexible cylinder polydisperse 0.15 + power	3000*	20*	1.68 ± 0.000782	**N/A**	**N/A**	2.55 ± 0.00251	26
Flexible cylinder polydisperse 0.15 + sphere	3000*	20*	2.49 ± 0.000711	**N/A**	4.11 ± 0.00122	**N/A**	74

Table S9. *SAXS fitting attempts for* ***PBI-I*** *as 10 mg/mL solutions pH = 5. *No fitting error available.*

Model	*Length / nm*	*Kuhn Length / nm*	*Cylinder Radius / nm*	*Axis Ratio*	*Sphere radius / nm*	*Power law*	X^2
Flexible elliptical cylinder	3000*	16.4 ± 0.0108	1.32 ± 0.00156	3.53 ± 0.00551	**N/A**	**N/A**	465
Flexible elliptical cylinder + power	3000*	20.3 ± 0.0152	1.26 ± 0.00148	3.89 ± 0.00577	**N/A**	5.41 ± 0.00826	37
Flexible elliptical cylinder + sphere	3000*	16.2 ± 0.0109	1.27 ± 0.00417	3.64 ± 0.0134	2.38 ± 0.0757	**N/A**	388
Flexible cylinder polydisperse 0.15	1560 ± 19.1	11.1 ± 0.00851	2.37 ± 0.000818	**N/A**	**N/A**	**N/A**	462
Flexible cylinder polydisperse 0.15 + power	3000*	3.18 ± 0.0153	1.49 ± 0.00122	**N/A**	**N/A**	7.02 ± 0.0117	244
Flexible cylinder polydisperse 0.15 + sphere	6750 ± 83.7	24.1 ± 0.0108	2.39 ± 0.000862	**N/A**	3.45 ± 0.00143	**N/A**	275

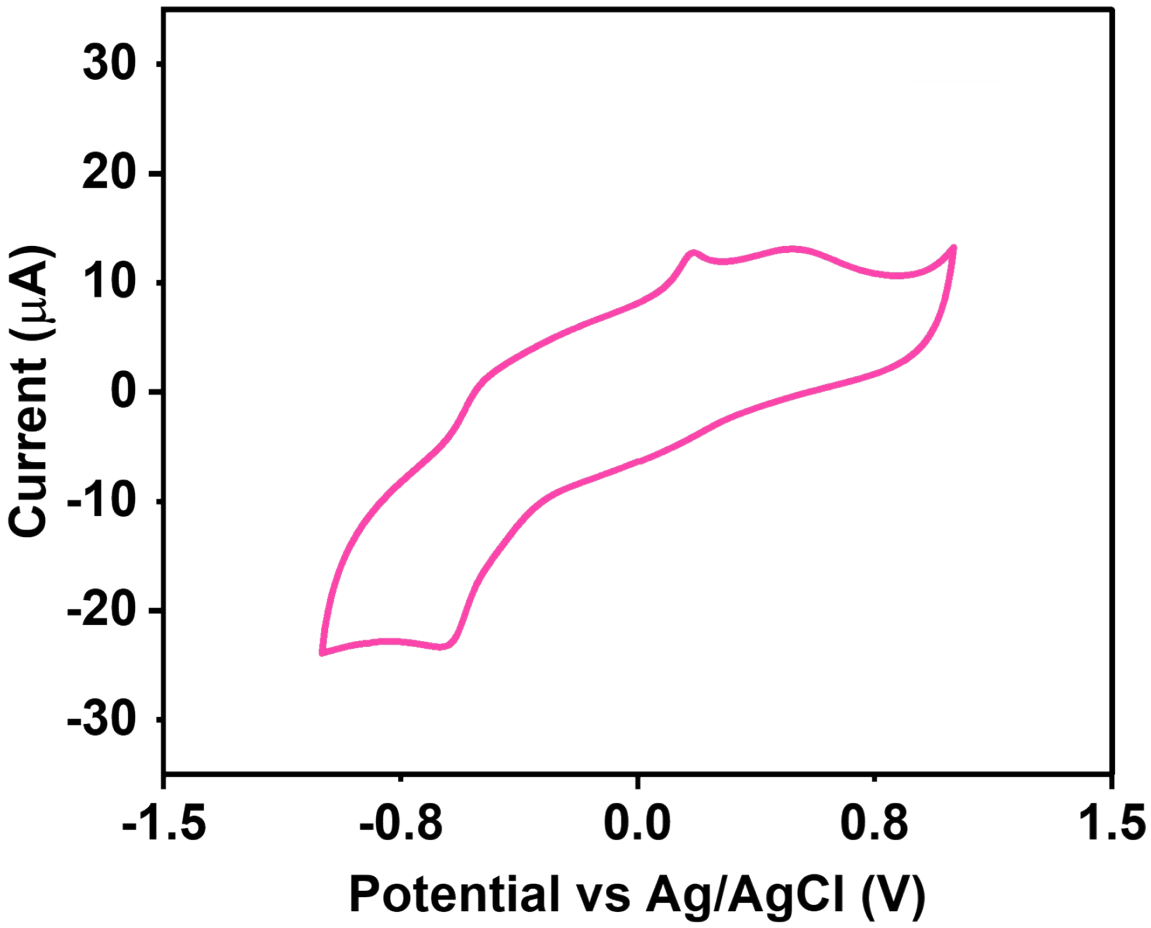

Figure S32. *Cyclic voltammogram of* ***PBI-L*** *(—) using 0.1 M NaCl electrolyte solution with a scan rate of 0.05 V/s.*

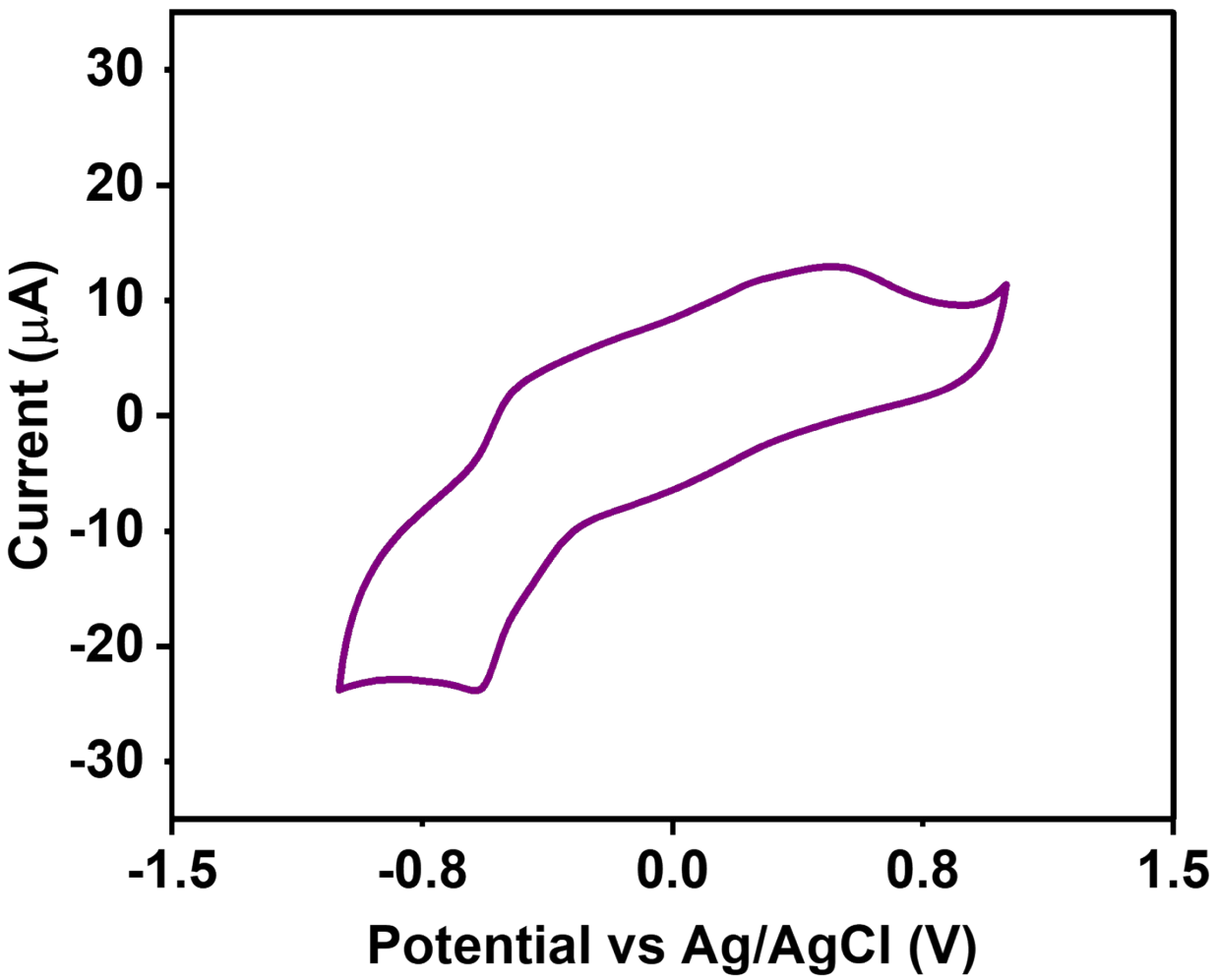

Figure S33. *Cyclic voltammogram of* ***PBI-I*** *(—) using 0.1 M NaCl electrolyte solution with a scan rate of 0.05 V/s.*

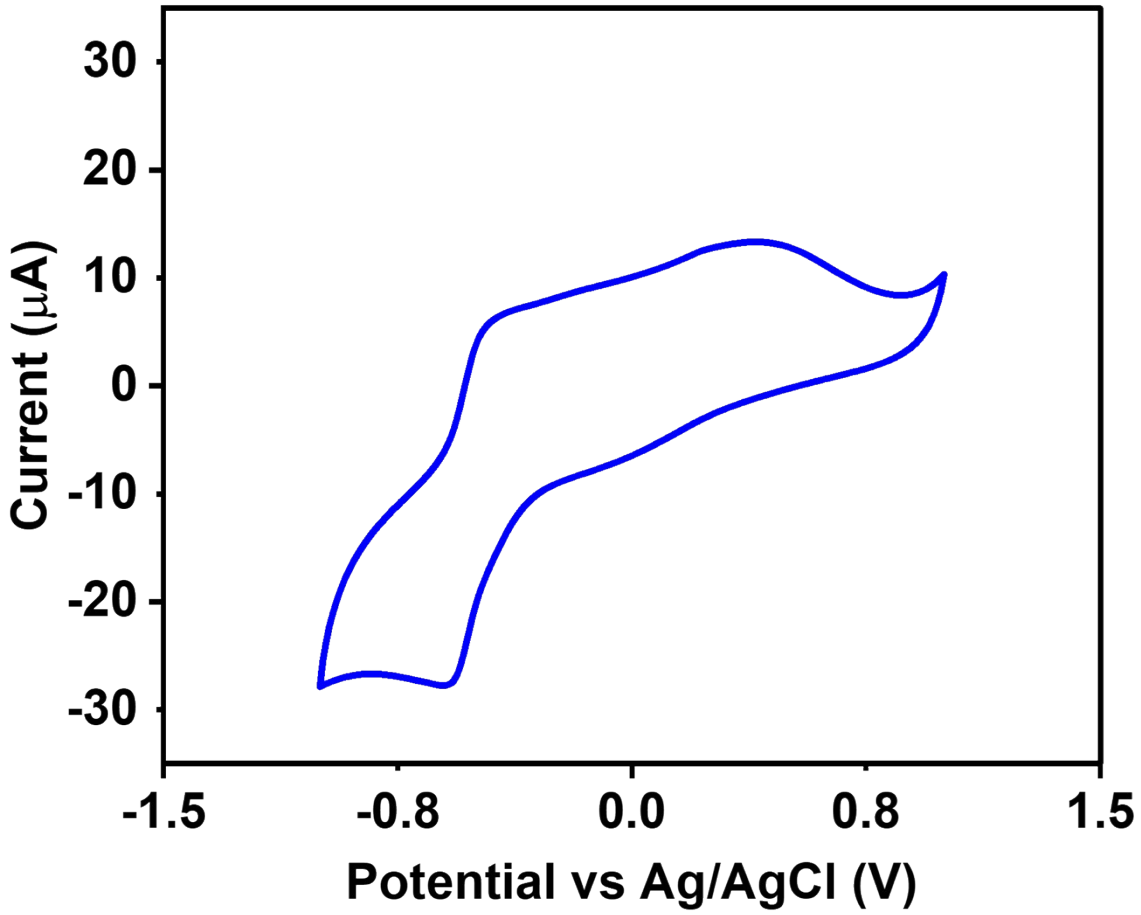

Figure S34. *Cyclic voltammogram of* ***PBI-V*** *(—) using 0.1 M NaCl electrolyte solution with a scan rate of 0.05 V/s.*

Table S10. *Reduction Potentials of PBIs in solution (10 mg/mL) at pH = 7*

	Reduction Potential (V)
PBI-L	-0.44 / -0.60
PBI-I	-0.42 / -0.57
PBI-V	-0.47 / -0.60

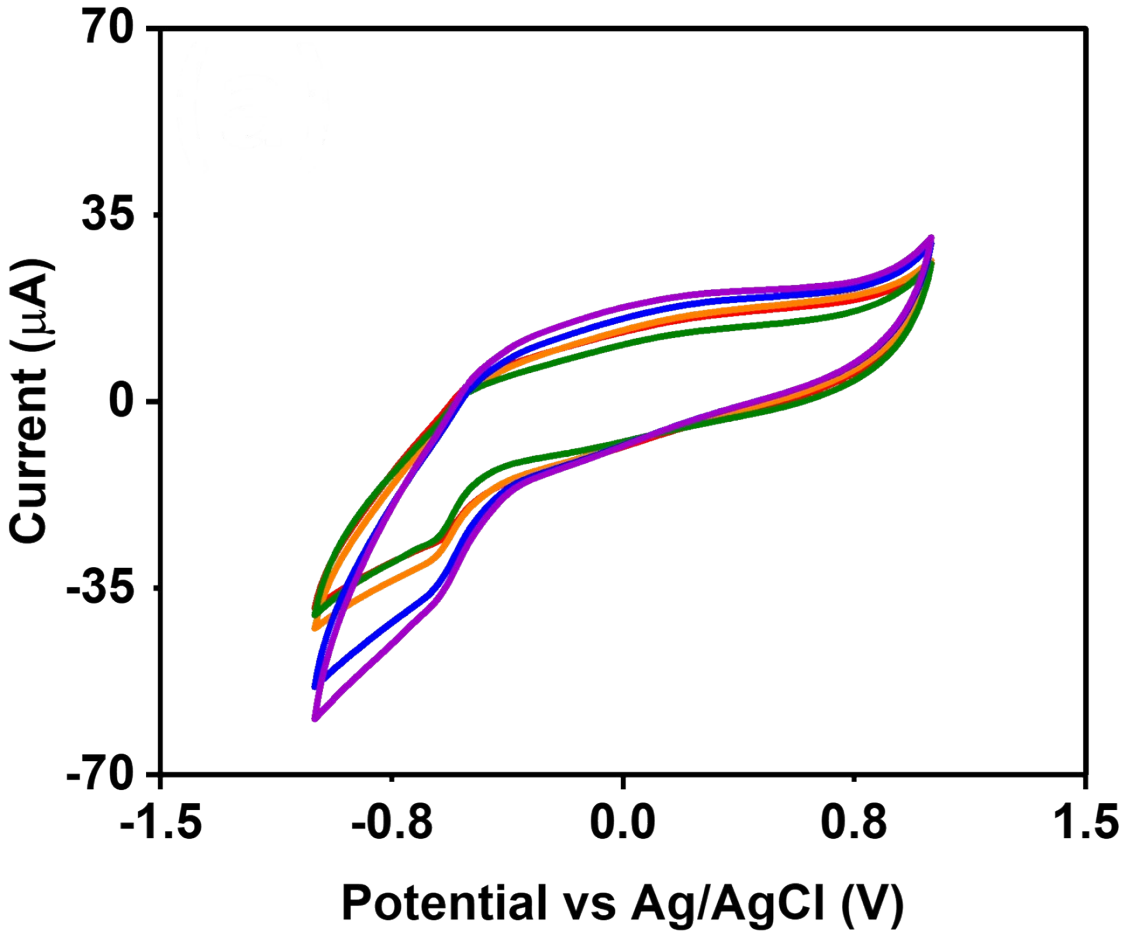

Figure S35. *Cyclic voltammograms of* ***PBI-L*** *using 0.1 M NaCl electrolyte solution with a scan rate of 0.05 V/s done at pH = 5 (—), pH = 6 (—), pH = 7 (—), pH = 8 (—), and pH = 9 (—).*

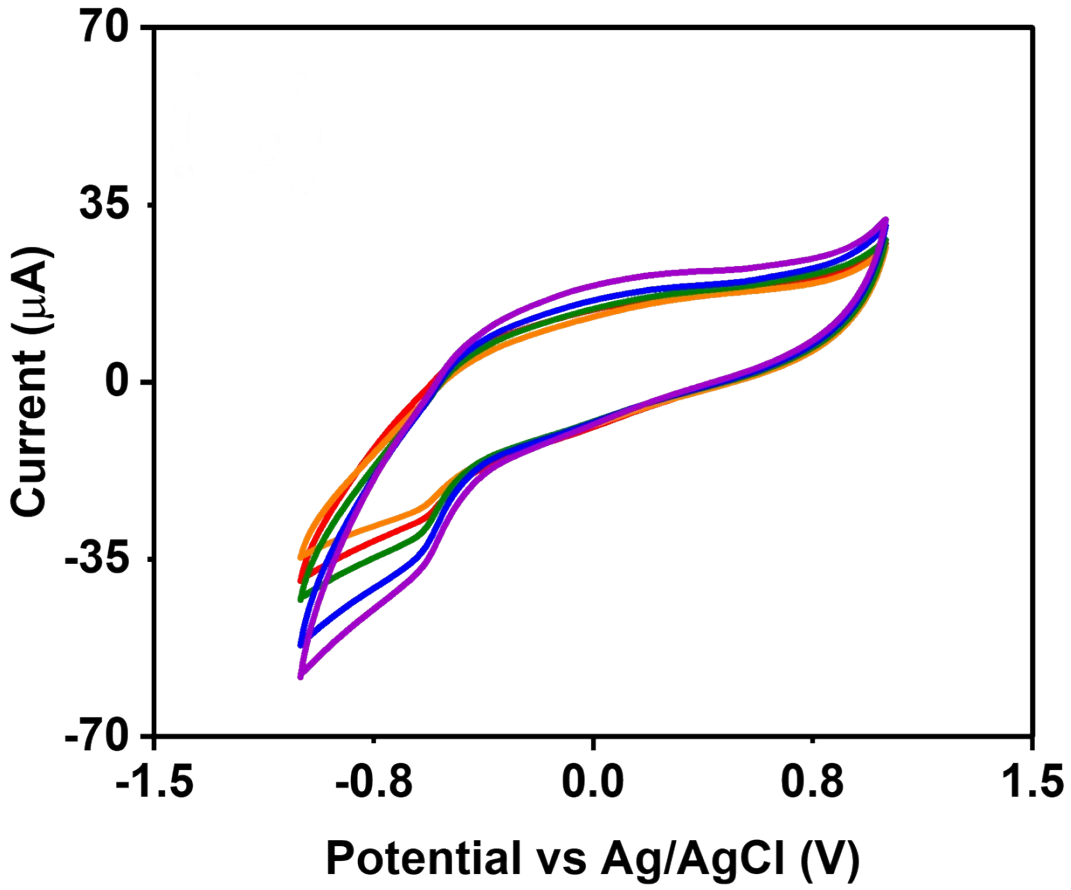

Figure S36. *Cyclic voltammograms of* ***PBI-I*** *using 0.1 M NaCl electrolyte solution with a scan rate of 0.05 V/s done at pH = 5 (—), pH = 6 (—), pH = 7 (—), pH = 8 (—), and pH = 9 (—).*

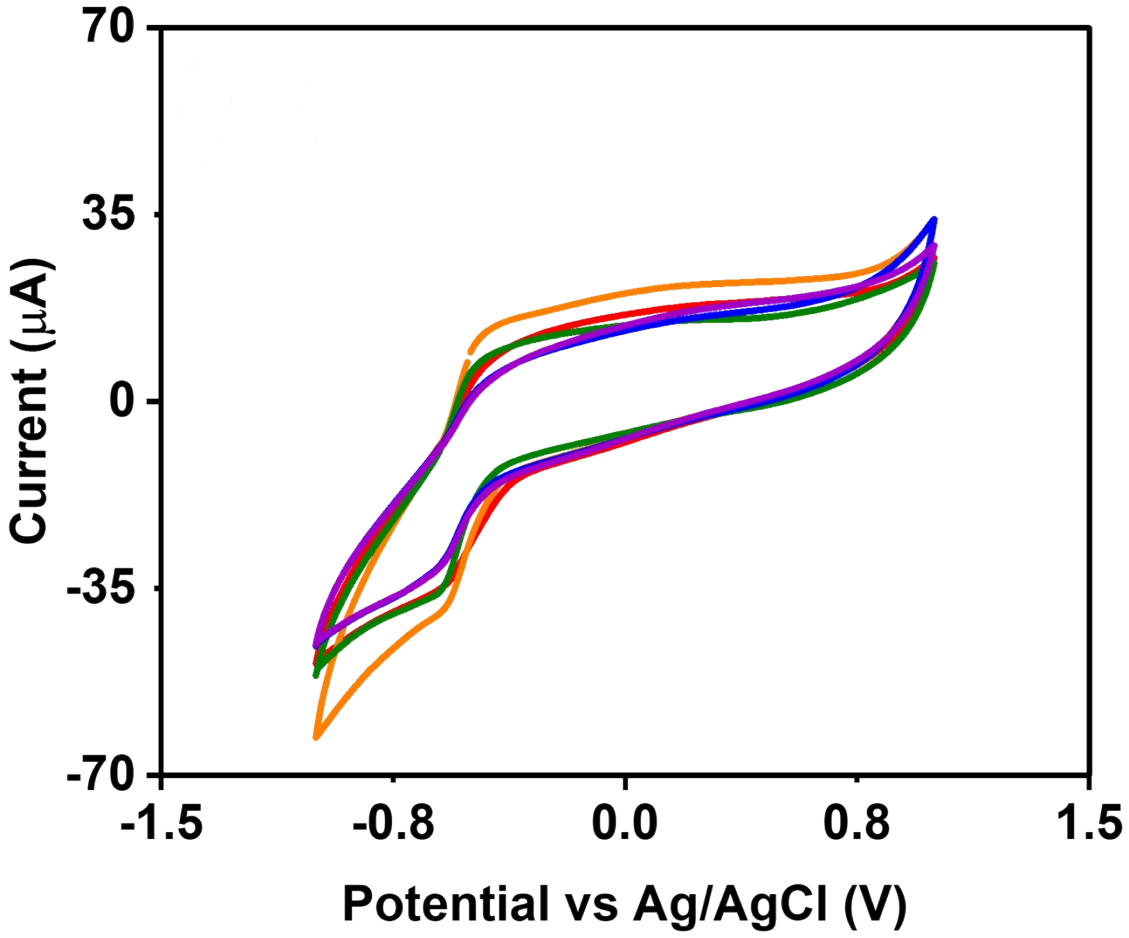

Figure S37. *Cyclic voltammograms of* ***PBI-V*** *using 0.1 M NaCl electrolyte solution with a scan rate of 0.05 V/s done at pH = 5 (—), pH = 6 (—), pH = 7 (—), pH = 8 (—), and pH = 9 (—).*

Table S11. *Reduction Potentials of PBIs in solution (10 mg/mL) at different pH*

	PBI-L	**PBI-I**	**PBI-V**
pH	Reduction Potentials (V)	Reduction Potentials (V)	Reduction Potentials (V)
5	-0.51 / -0.58	-0.49 / -0.57	-0.49 / -0.57
6	-0.47 / -0.61	-0.47 / -0.58	-0.45 / -0.58
7	-0.51 / -0.61	-0.51 / -0.56	-0.51 / -0.58
8	-0.49 / -0.62	-0.51 / -0.58	-0.51 / -0.59
9	-0.49 / -0.59	-0.49 / -0.58	-0.51 / -0.59

3.3 Hydrogel Characterization

Table S12. *pH of PBIs before and after gelation*

PBI	**L**	**I**	**V**
pH before gelation	6.6	6.8	6.8
pH after gelation	3.7	3.7	3.7

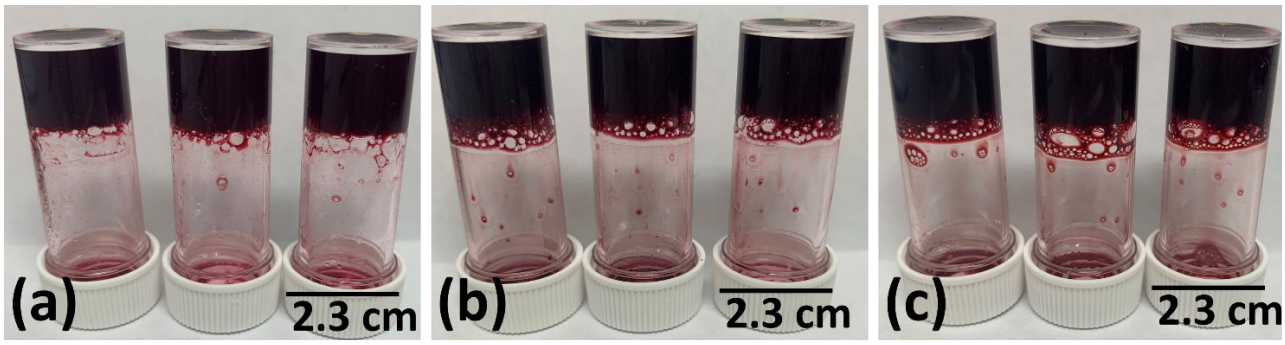

Figure S35. *Pictures of inverted Sterlin vials showing hydrogel containing (a)* ***PBI-L*** *(b)* ***PBI-I*** *(c)* ***PBI-V***

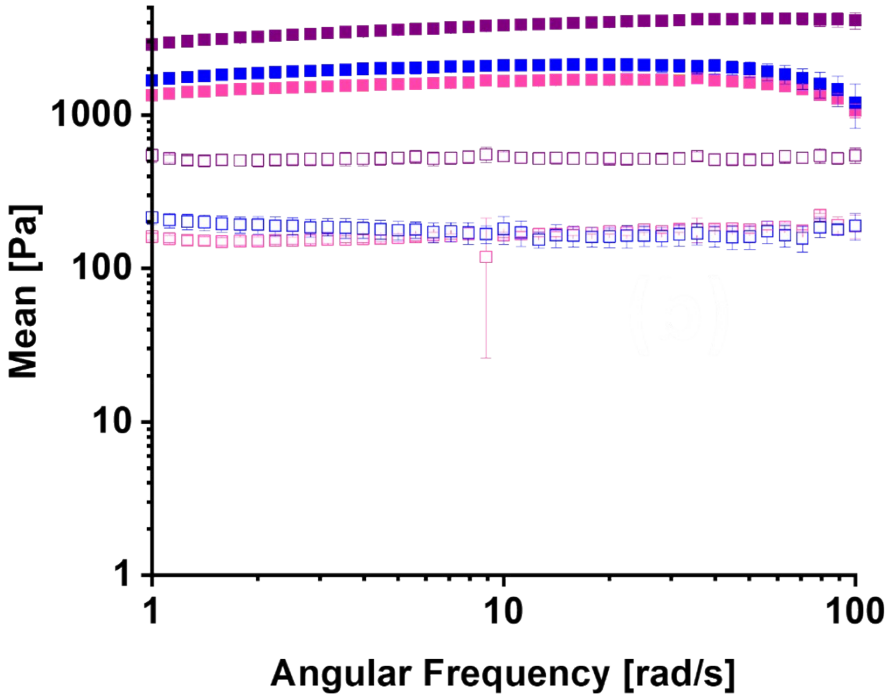

Figure S39. *Frequency Sweep data for* ***PBI-L*** *(**pink**),* ***PBI-I*** *(**purple**) and* ***PBI-V*** *(**blue**). In all cases, the storage modulus (G') is represented by the closed symbols and the loss modulus (G") is represented by open symbols. Measurements were performed in duplicated and errors were calculated from the standard deviation of 3 repeat measurements.*

Table S13. *S_0-S_1 ratio for PBIs hydrogels at a concentration of 10 mg/mL using a GdL trigger before and after irradiation*

PBI	S_0-S_1 ratio for solutions before irradiation	S_0-S_1 ratio for solutions after irradiation
L	0.55	0.59
I	0.50	0.58
V	0.69	0.77

Table S14. *SAXS fitting results for **PBI-L** as solutions (**top**) and hydrogels (**bottom**) at 10 mg/mL. *No fitting error available.*

Model	*Length / nm*	*Kuhn Length / nm*	*Cylinder Radius / nm*	*Axis Ratio*	*Sphere radius / nm*	*Power law*	*X^2*
Flexible elliptical cylinder + sphere	*400 ± 9.06*	*10.1 ± 0.299*	*0.958 ± 0.0235*	*7.46 ± 0.161*	*2.48 ± 0.0142*	***N/A***	*3.3*
Flexible elliptical cylinder + power	*3000**	*15.2 ± 0.138*	*3.57 ± 0.00938*	*2.23 ± 0.121*	***N/A***	*2.76 0.00441*	*1.4*

Table S15. *SAXS fitting results for **PBI-I** as solutions (**top**) and hydrogels (**bottom**) at 10 mg/mL. *No fitting error available.*

Model	*Length / nm*	*Kuhn Length / nm*	*Cylinder Radius / nm*	*Axis Ratio*	*Sphere radius / nm*	*Power law*	*X^2*
Flexible cylinder + power	*86.0 ± 0.00916*	*8.61 ± 0.321*	*5.16 ± 0.0458*	***N/A***	***N/A***	*1.21 ± 0.0395*	*1.0*
Flexible elliptical cylinder + power	*332 ± 12.5*	*30.6 ± 1.27*	*3.36 ± 0.00881*	*2.38 ± 0.0106*	***N/A***	*2.31 ± 0.0149*	*2.3*

Table S16. *SAXS fitting results for* ***PBI-V*** *as solutions (t**op**) and hydrogels (**bottom**) at 10 mg/mL. *No fitting error available.*

Model	*Length / nm*	*Kuhn Length / nm*	*Cylinder Radius / nm*	*Axis Ratio*	*Sphere radius / Å*	*Power law*	*X^2*
Flexible cylinder polydisperse 0.15 + power	*154 ± 6.27*	*5.51 ± 0.342*	*4.36 ± 0.0242*	***N/A***	***N/A***	*1.99 ± 0.0128*	*2.1*
Flexible elliptical cylinder polydisperse 0.3	*426 ± 6.49*	*3.2 ± 0.323*	*2.73 ± 0.00262*	*3.51 ± 0.0146*	***N/A***	***N/A***	*3.4*

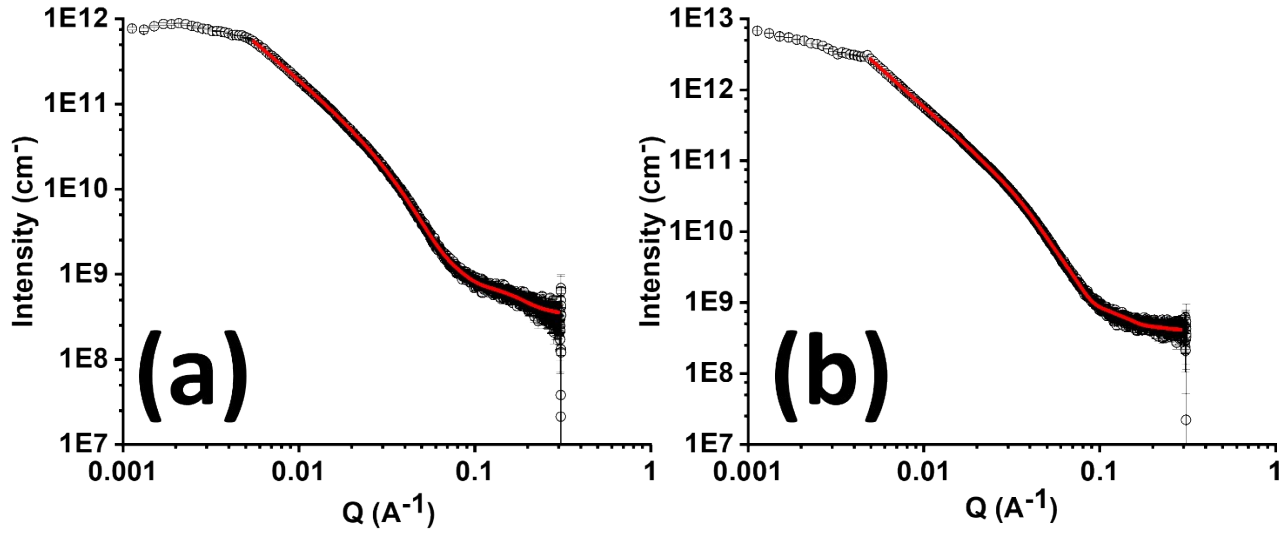

Figure S40. *SAXS data for* ***PBI-L*** *showing scattering vector vs scattering intensity (open black circles) with the corresponding model fits (solid red lines). (a) 10 mg/mL solutions (b) hydrogels.*

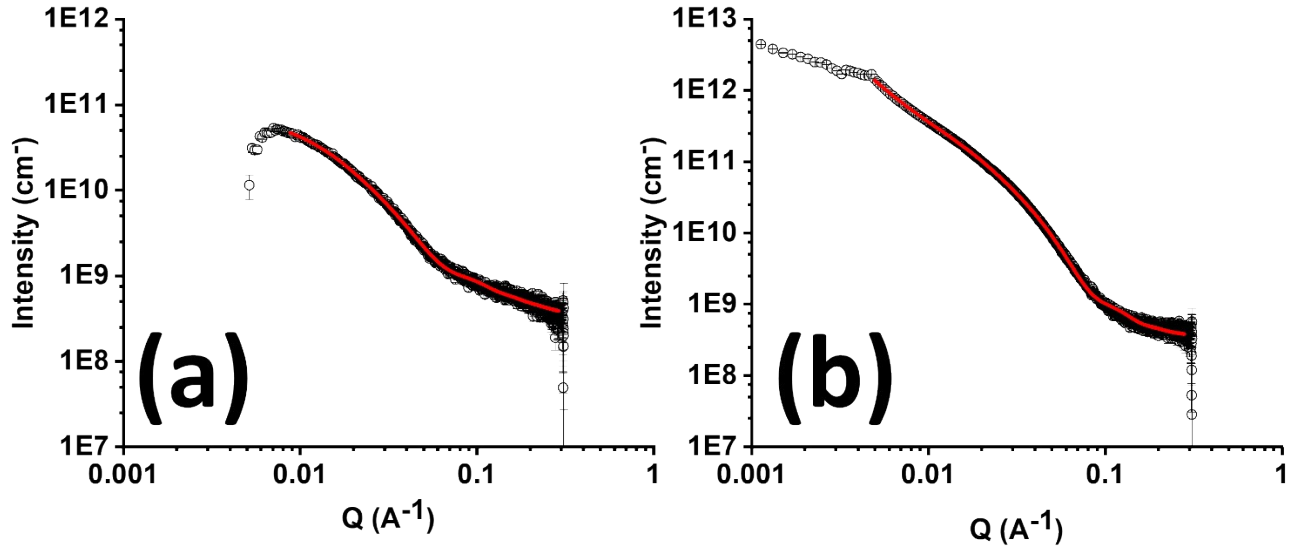

Figure S41. *SAXS data for* ***PBI-I*** *showing scattering vector vs scattering intensity (open black circles) with the corresponding model fits (solid red lines). (a) 10 mg/mL solutions (b) hydrogels.*

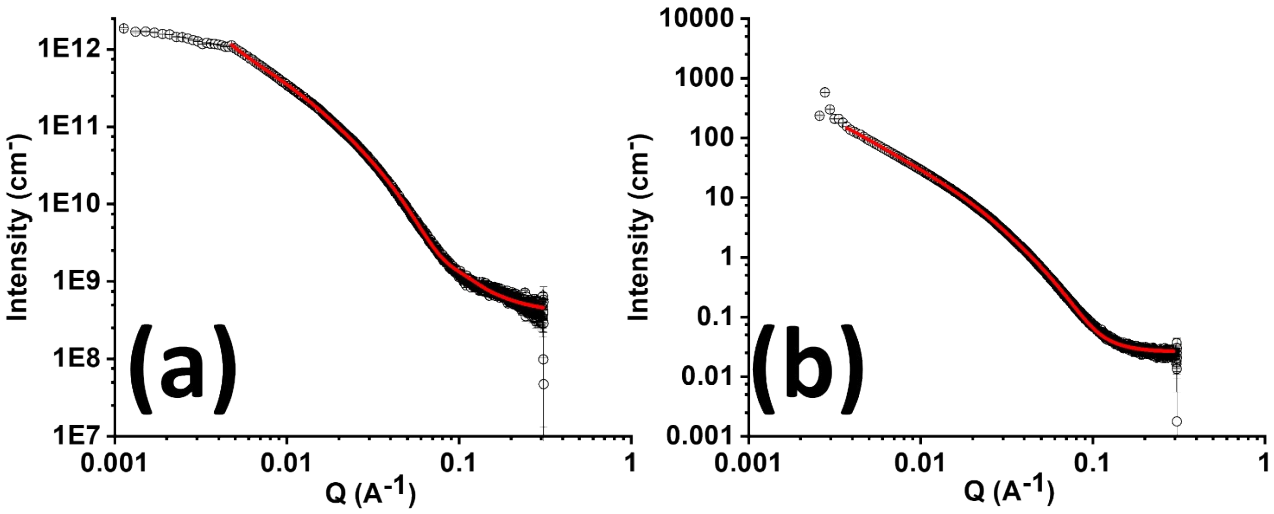

Figure S42. *SAXS data for* ***PBI-V*** *showing scattering vector vs scattering intensity (open black circles) with the corresponding model fits (solid red lines). (a) 10 mg/mL solutions (b) hydrogels.*

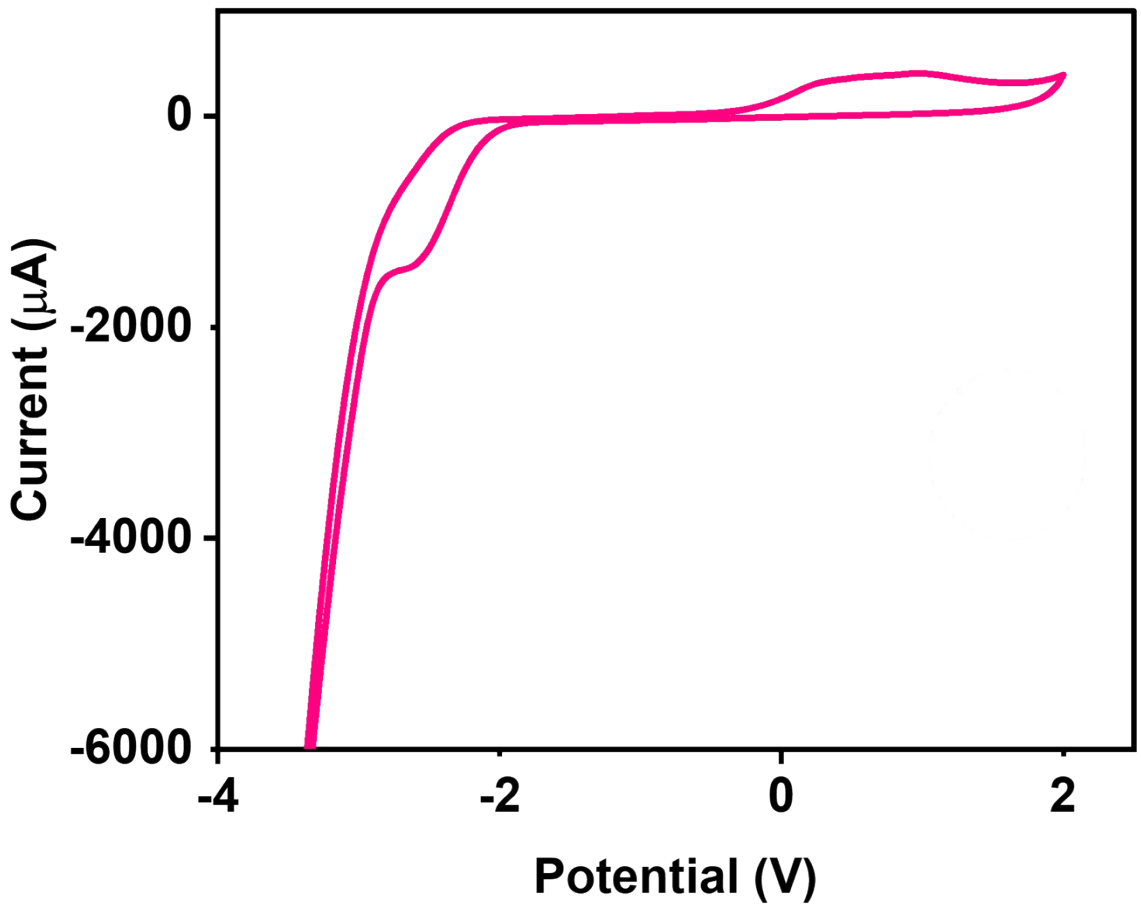

Figure S43. *Cyclic voltammogram of* ***PBI-L*** *(—) hydrogels using 0.1 M NaCl electrolyte solution with a scan rate of 0.1 V/s.*

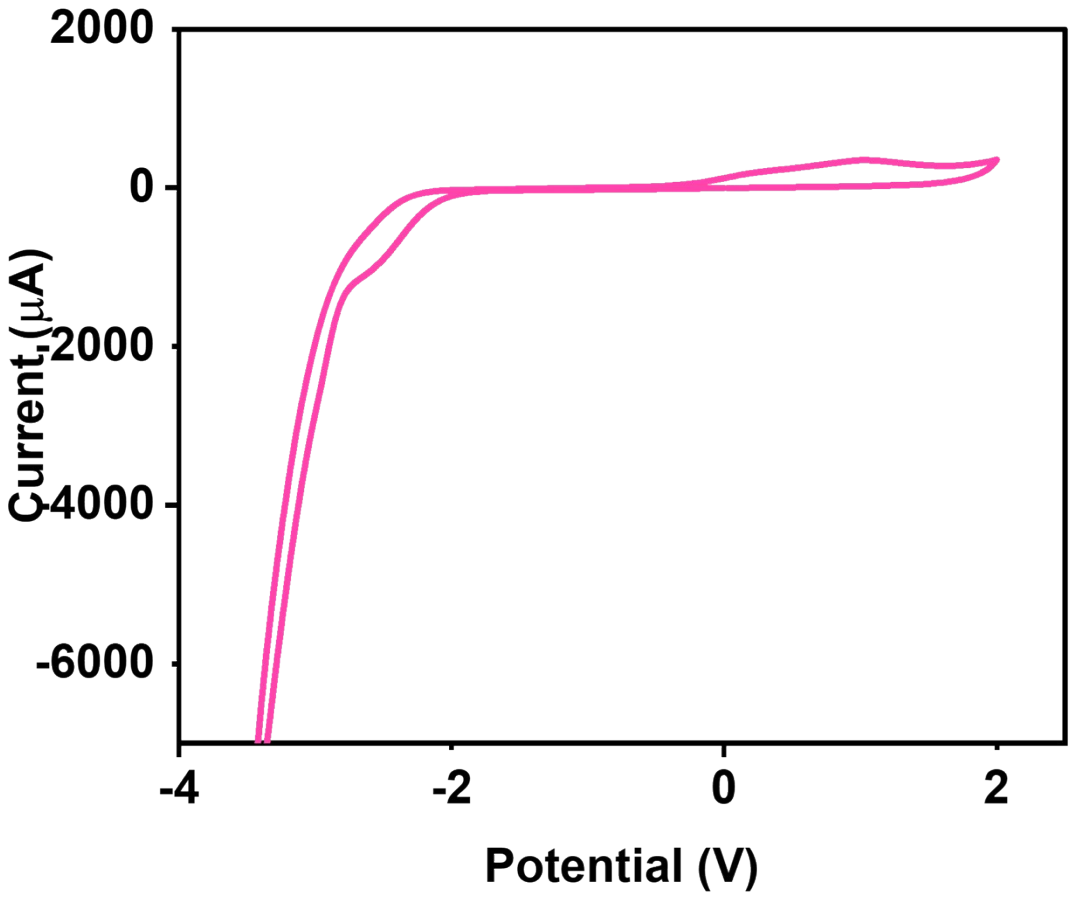

Figure S44. *Cyclic voltammogram of* ***PBI-L*** *(—) hydrogels using 0.1 M NaCl electrolyte solution with a scan rate of 0.05 V/s.*

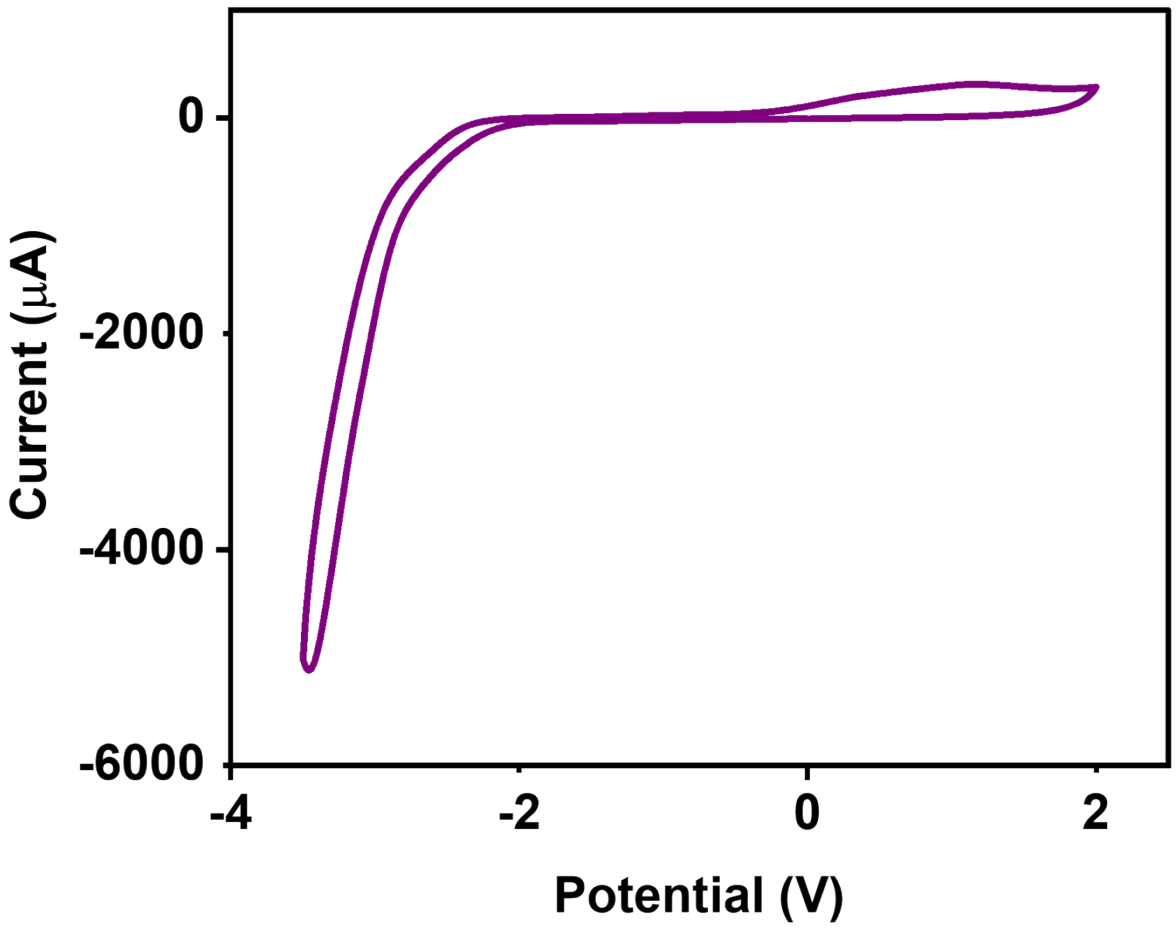

Figure S45. *Cyclic voltammogram of* ***PBI-I*** *(—) hydrogels using 0.1 M NaCl electrolyte solution with a scan rate of 0.1 V/s.*

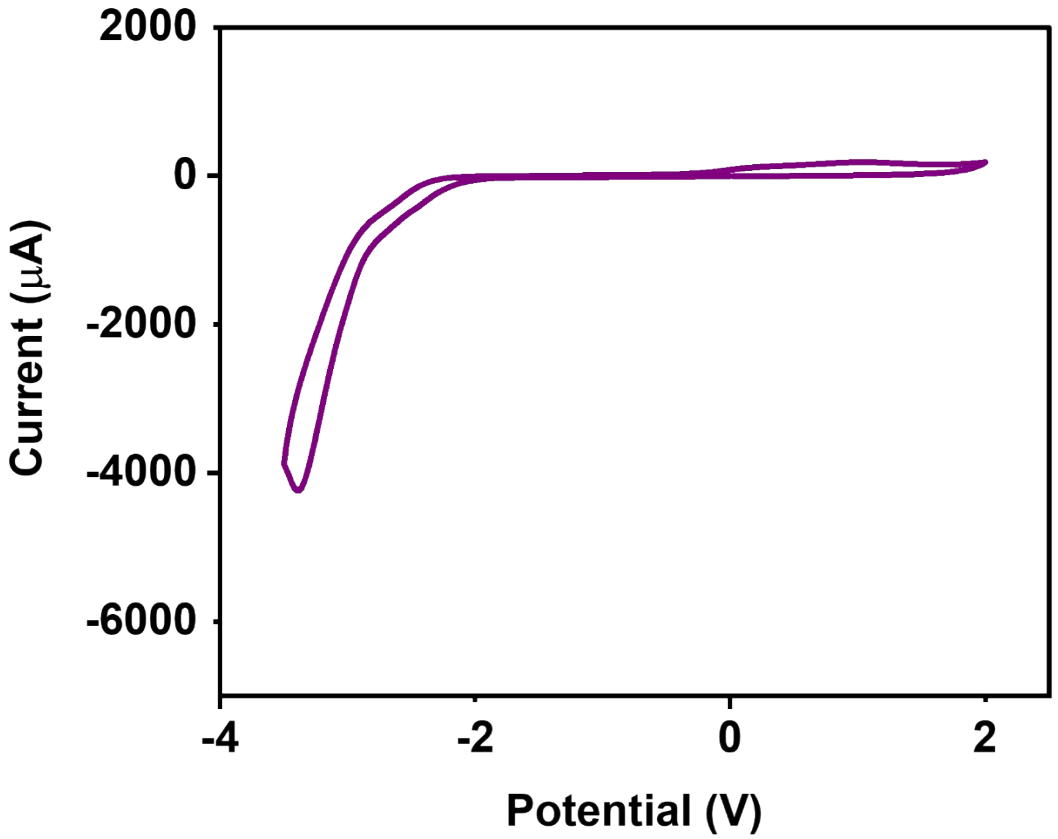

Figure S46. *Cyclic voltammogram of* ***PBI-I*** *(—) hydrogels using 0.1 M NaCl electrolyte solution with a scan rate of 0.05 V/s.*

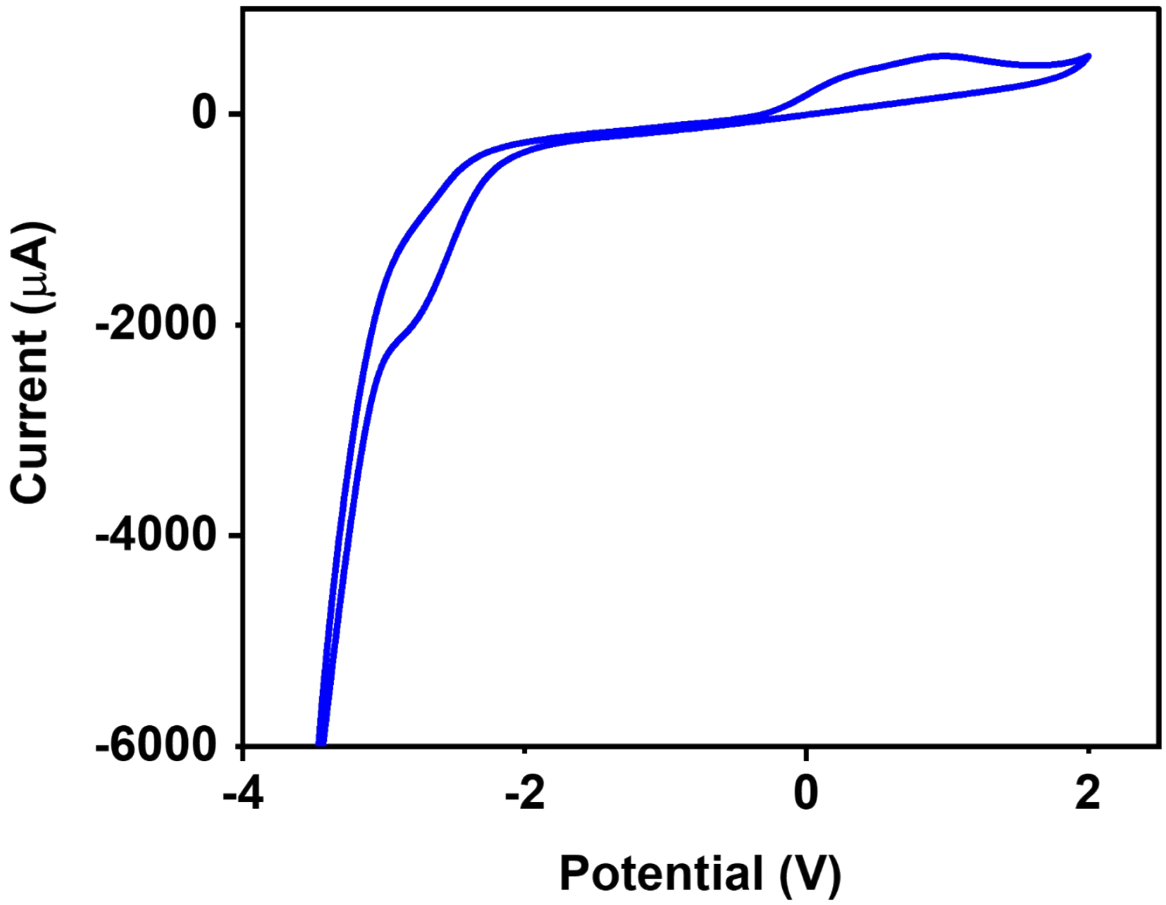

Figure S47. *Cyclic voltammogram of* ***PBI-V*** *(—) hydrogels using 0.1 M NaCl electrolyte solution with a scan rate of 0.1 V/s.*

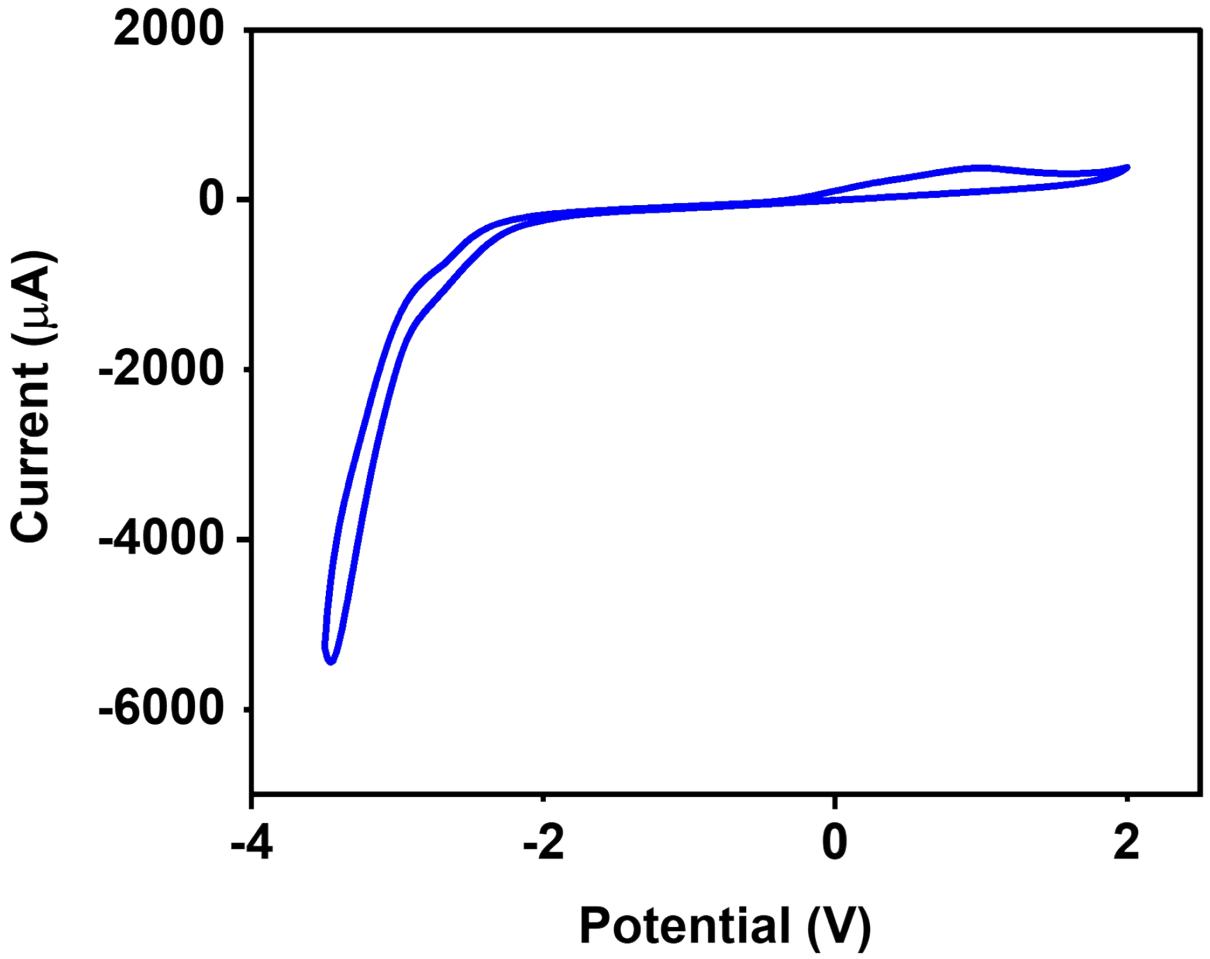

Figure S48. *Cyclic voltammogram of* ***PBI-V*** *(—) hydrogels using 0.1 M NaCl electrolyte solution with a scan rate of 0.05 V/s.*

3.3 Kinetics

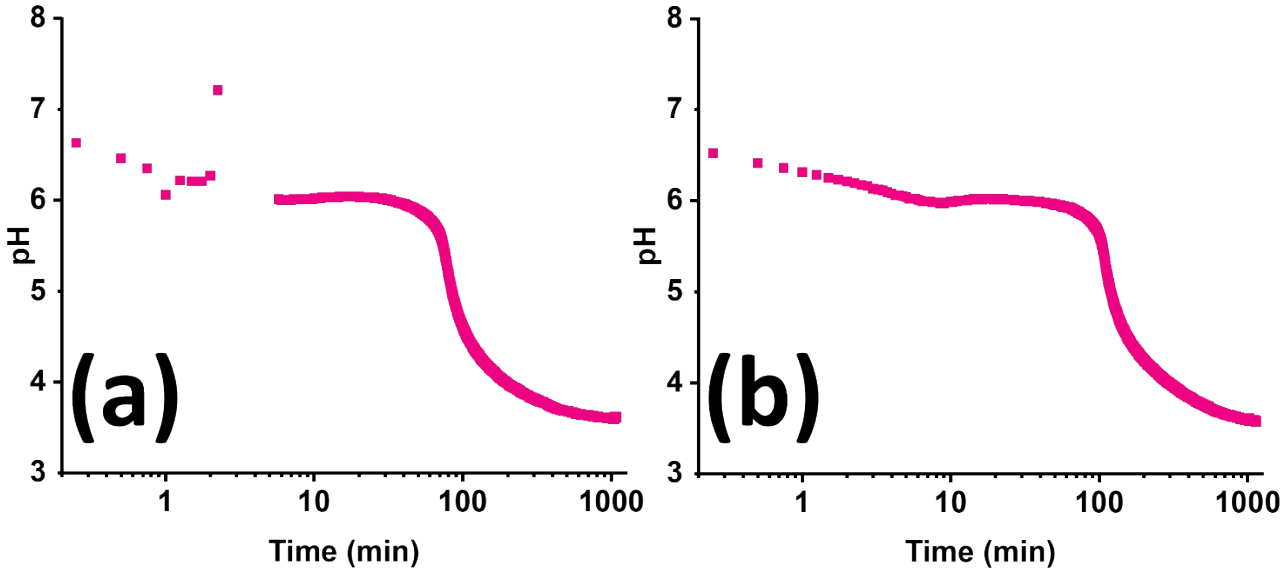

Figure S49. *Change in pH over time for* ***PBI-L*** *with GdL at* ***(a)*** *25 °C and* ***(b)*** *20 °C*

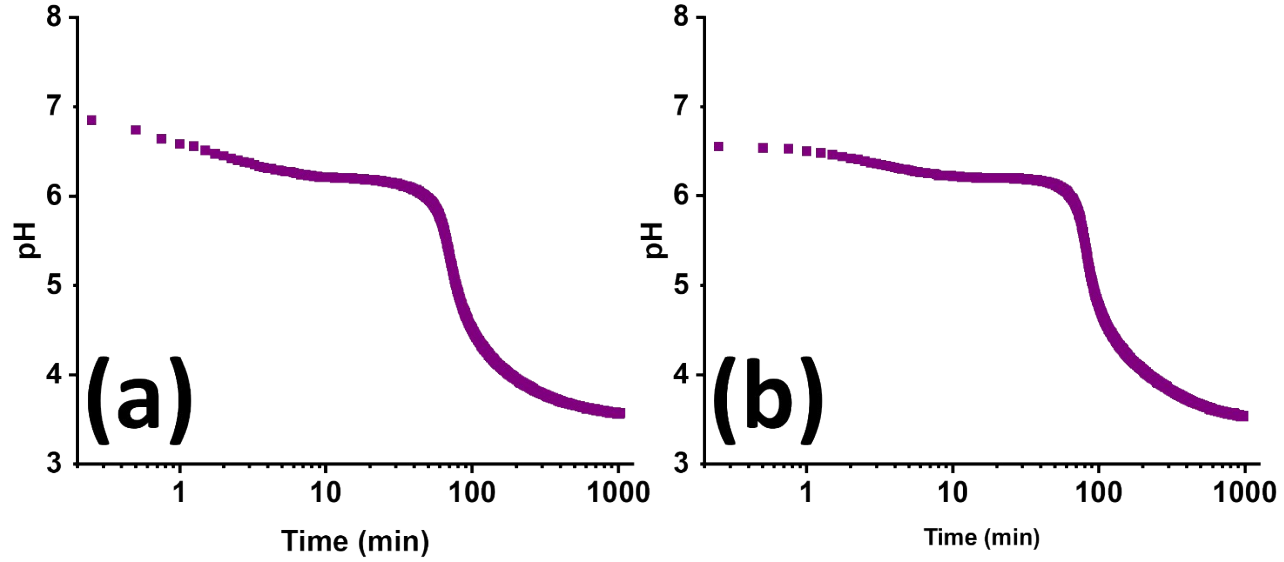

Figure S50. *Change in pH over time for* ***PBI-I*** *with GdL at* ***(a)*** *25 °C and* ***(b)*** *20 °C*

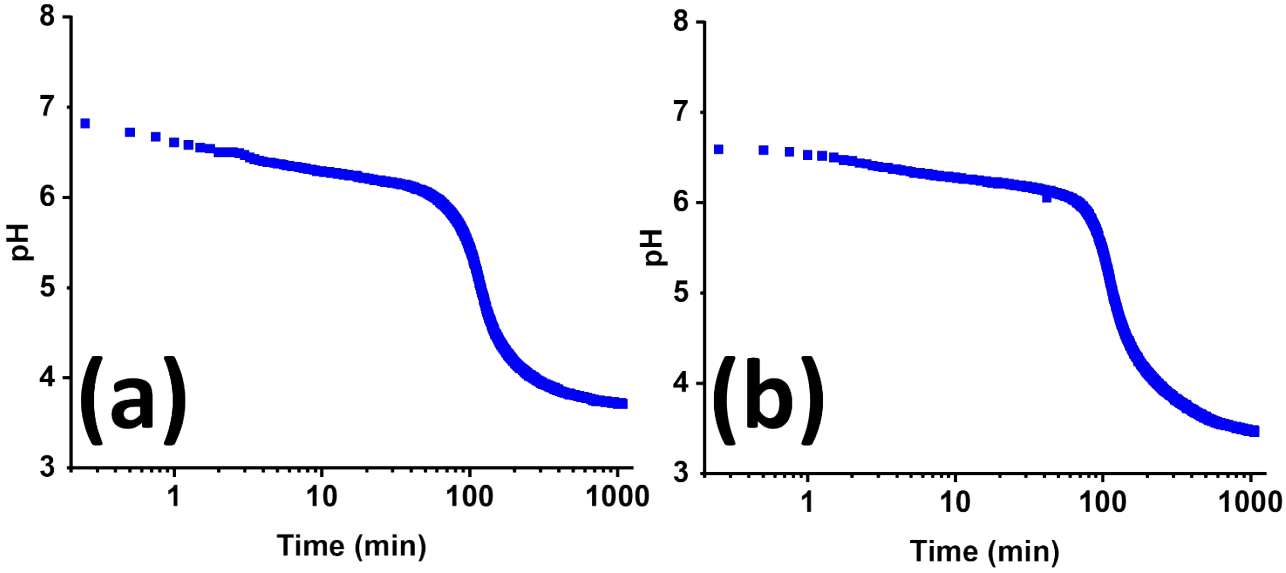

Figure S51. *Change in pH over time for PBI-V with GdL at (a) 25 °C and (b) 20 °C*

Table S17. *Summarized data from pH change over time with GdL and different PBIs*

	PBI-L		**PBI-I**		**PBI-V**	
	25 °C	20 °C	25 °C	20 °C	25 °C	20 °C
pK_{a1}	N/A	6.41	6.85	6.55	6.82	6.59
pK_{a2}	6.04	6.01	6.19	6.2	6.24	6.24

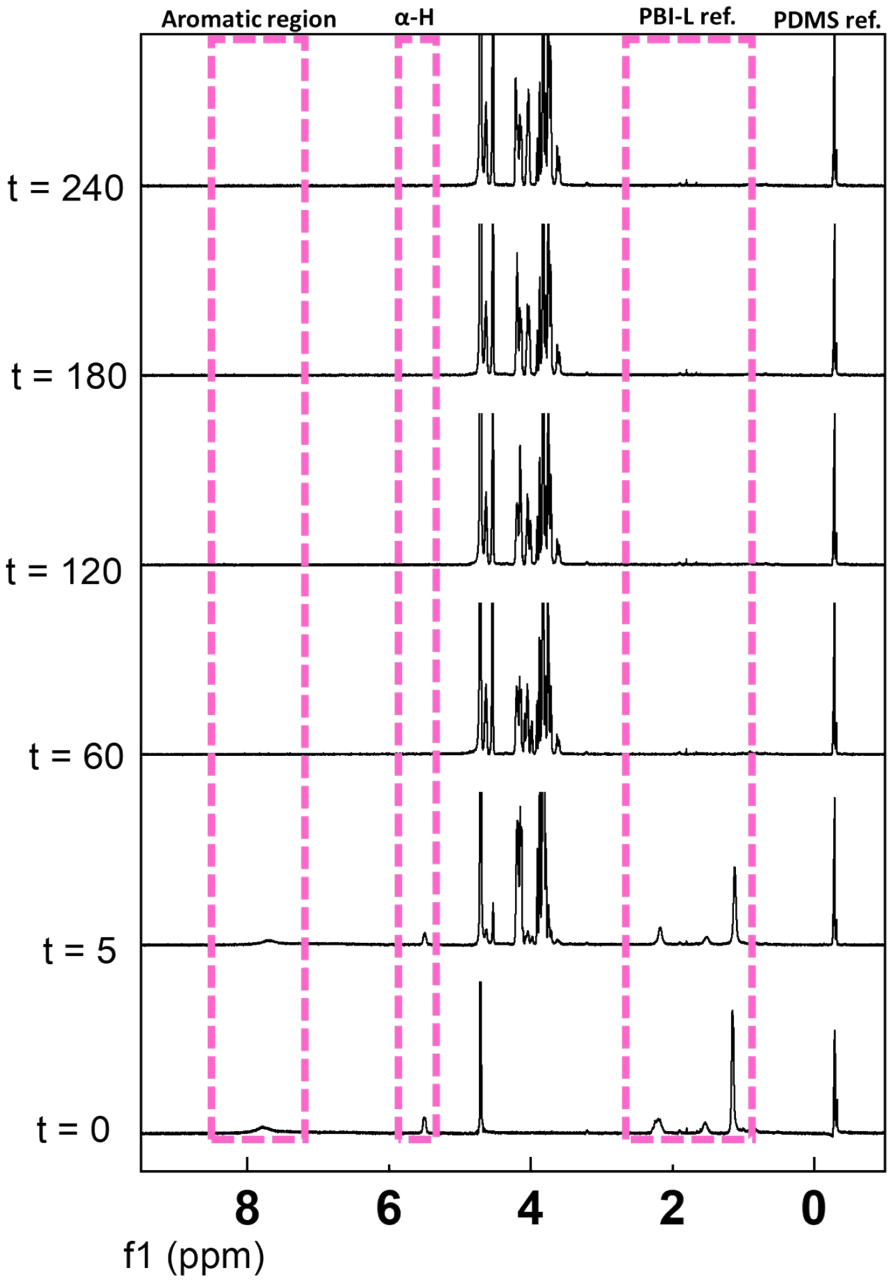

Figure S52. *^{1}H NMR spectra recorded over time after the addition of GdL to a solution of* ***PBI-L*** *in D_2O/NaOD. The time (in minutes) at which the data were collected is shown on the left, with the peaks corresponding to* ***PBI-L*** *being highlighted in pink. The peaks between around 3.5 and 4.3 ppm are from GdL and its hydrolysis products (mainly gluconic acid). The peak at 4.5 ppm is from the solvent. The methyl groups from the PDMS standard against which the peaks of* ***PBI-L*** *are integrated are at -0.5 ppm. The proton environment labelled* ***PBI-L*** *ref. was used to determine the percentage assembly over time.*

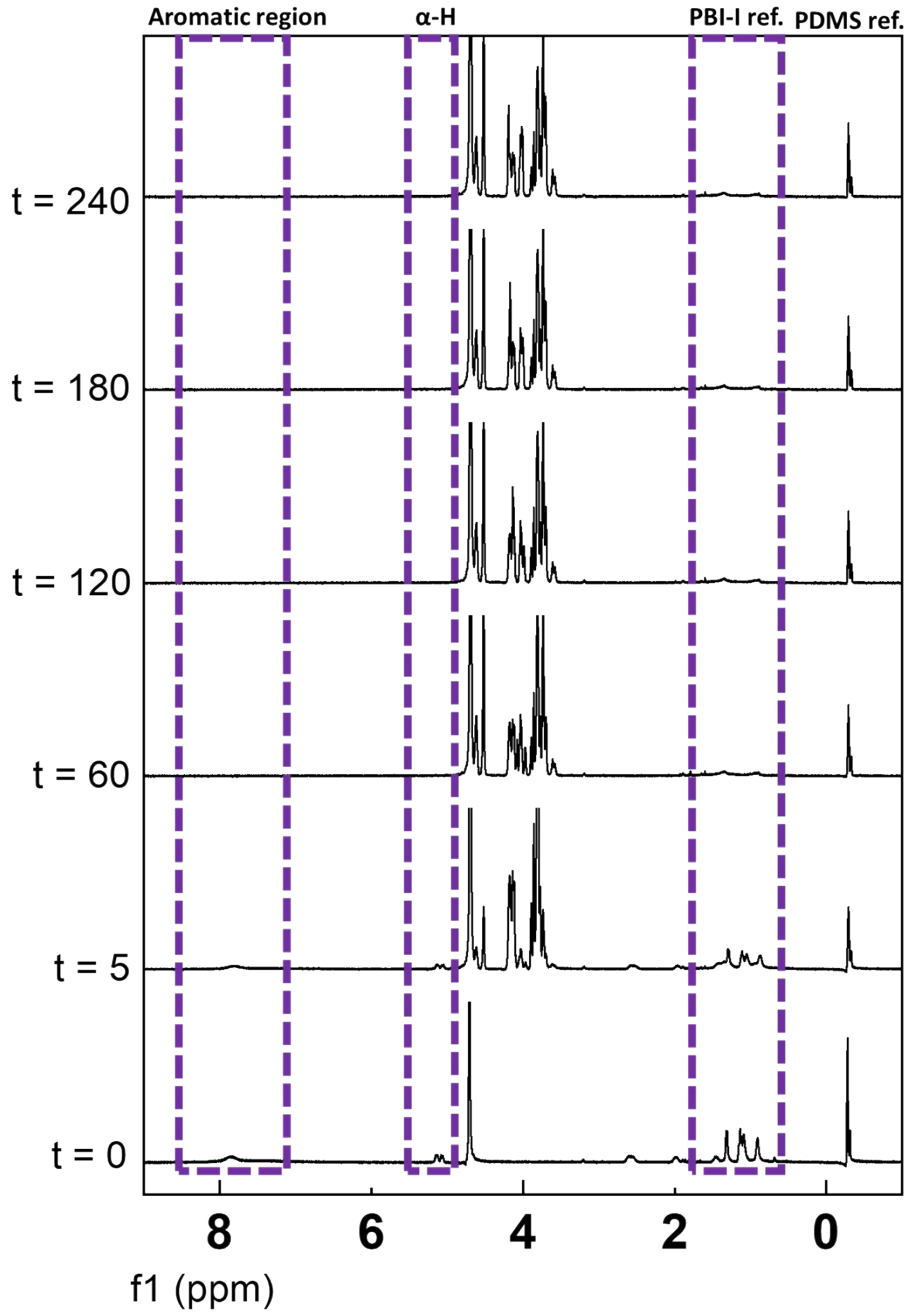

Figure S53. *^{1}H NMR spectra recorded over time after the addition of GdL to a solution of **PBI-I** in D_2O/NaOD. The time (in minutes) at which the data were collected is shown on the left, with the peaks corresponding to **PBI-I** being highlighted in purple. The peaks between around 3.5 and 4.3 ppm are from GdL and its hydrolysis products (mainly gluconic acid). The peak at 4.5 ppm is from the solvent. The methyl groups from the PDMS standard against which the peaks of **PBI-I** are integrated are at -0.5 ppm. The proton environment labelled **PBI-I** ref. was used to determine the percentage assembly over time.*

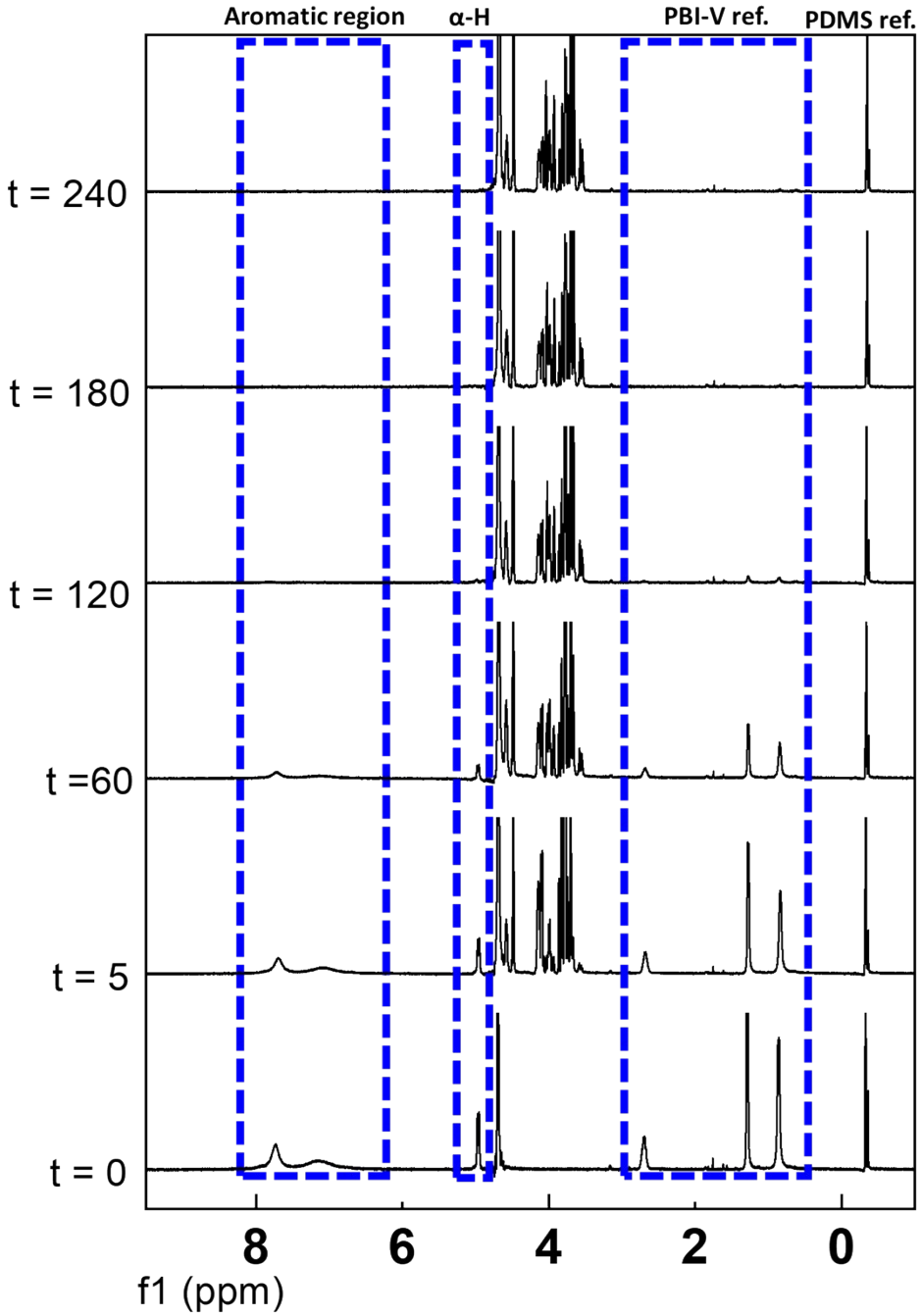

Figure S54. *^{1}H NMR spectra recorded over time after the addition of GdL to a solution of **PBI-V** in D_2O/NaOD. The time (in minutes) at which the data were collected is shown on the left, with the peaks corresponding to **PBI-V** being highlighted in blue. The peaks between around 3.5 and 4.3 ppm are from GdL and its hydrolysis products (mainly gluconic acid). The peak at 4.5 ppm is from the solvent. The methyl groups from the PDMS standard against which the peaks of **PBI-V** are integrated are at -0.5 ppm. The proton environment labelled **PBI-V** ref. was used to determine the percentage assembly over time.*

4. References

1 M. J. Farooqi, M. A. Penick, J. Burch, G. R. Negrete and L. Brancaleon, *Spectrochim. Acta - Part A Mol. Biomol. Spectrosc.*, 2016, **153**, 124–131.

2 Y. Xu, S. Leng, C. Xue, R. Sun, J. Pan, J. Ford and S. Jin, *Angew. Chemie - Int. Ed.*, 2007, **46**, 3896–3899.

3 E. R. Draper, J. J. Walsh, T. O. McDonald, M. A. Zwijnenburg, P. J. Cameron, A. J. Cowan and D. J. Adams, *J. Mater. Chem. C*, 2014, **2**, 5570–5575.

4 N. B. Bowden, K. A. Willets, W. E. Moerner and R. M. Waymouth, *Macromolecules*, 2002, **35**, 8122–8125.

5 J. Filik, A. W. Ashton, P. C. Y. Chang, P. A. Chater, S. J. Day, M. Drakopoulos, M. W. Gerring, M. L. Hart, O. V Magdysyuk, S. Michalik, A. Smith, C. C. Tang, N. J. Terrill, M. T. Wharmby and H. Wilhelm, *J. Appl. Crystallogr.*, 2017, **50**, 959–966.

6 B. R. Pauw, A. J. Smith, T. Snow, N. J. Terrill and A. F. Thünemann, *J. Appl. Crystallogr.*, 2017, **50**, 1800–1811.

7 P. Kienzle, NIST Neutron Activation and Scattering Calculator, https://www.ncnr.nist.gov/resources/activation/.

8 Sasview, *http://www.sasview.org/.*

9 M. C. Nolan, J. J. Walsh, L. L. E. Mears, E. R. Draper, M. Wallace, M. Barrow, B. Dietrich, S. M. King, A. J. Cowan and D. J. Adams, *J. Mater. Chem. A*, 2017, **5**, 7555–7563.

10 D. McDowall, B. J. Greeves, R. Clowes, K. McAulay, A. M. Fuentes-Caparrós, L. Thomson, N. Khunti, N. Cowieson, M. C. Nolan, M. Wallace, A. I. Cooper, E. R. Draper, A. J. Cowan and D. J. Adams, *Adv. Energy Mater.*, 2020, **2002469**, 1–10.

11 E. R. Draper, L. J. Archibald, M. C. Nolan, R. Schweins, M. A. Zwijnenburg, S. Sproules and D. J. Adams, *Chem. - A Eur. J.*, 2018, **24**, 4006–4010.

12 E. R. Cross, S. Sproules, R. Schweins, E. R. Draper and D. J. Adams, 2018, 8–11.